An Eulerian-Lagrangian localized adjoint method for the advection-diffusion equation

Michael A. Celia

Water Resources Program, Dept. of Civil Engineering and Operations Research, Princeton University, Princeton, NJ 08544, U.S.A.

Thomas F. Russell

Department of Mathematics, University of Colorado at Denver, Denver, CO 80204-5300, U.S.A.

Ismael Herrera

Instituto de Geofísica, UNAM, Apdo. Postal 22-582, 14000 Mexico D.F., Mexico

Richard E. Ewing

Deparment of Mathematics, University of Wyoming, Laramie, WY 82071, U.S.A.

Many numerical methods use characteristic analysis to accommodate the advective component of transport. Such characteristic methods include Eulerian-Lagrangian methods (ELM), modified method of characteristics (MMOC), and operator splitting methods. A generalization of characteristic methods can be developed using an approach that we refer to as an Eulerian-Lagrangian localized adjoint method (ELLAM). This approach is a space-time extension of the optimal test function (OTF) method. The method provides a consistent formulation by defining test functions as specific solutions of the localized homogeneous adjoint equation. All relevant boundary terms arise naturally in the ELLAM formulation, and a systematic and complete treatment of boundary condition implementation results. This turns out to have significant implications for the calculation of boundary fluxes. An analysis of global mass conservation leads to the final ELLAM approximation, which is shown to possess the conservative property. Numerical calculations demonstrate the behaviour of the method with emphasis on treatment of boundary conditions. Discussion of the method includes ideas on extensions to higher spatial dimensions, reactive transport, and variable coefficient equations.

1. INTRODUCTION

Advection-diffusion transport equations are important in many branches of engineering and applied science. These equations are characterized by a nondissipative (hyperbolic) advective transport component and a dissipative (parabolic) diffusive component. When diffusion is the dominant process, virtually all numerical solution procedures perform well. However, when advection is the dominant transport process, most numerical procedures exhibit some combination of excessive nonphysical oscillations and excessive numerical diffusion. While this behaviour is easily explained using, for example, general Fourier analysis[41], the development of numerical schemes that overcome the problems is an ongoing challenge. While extremely fine mesh refinement is one possible solution, it is usually not a feasible alternative due to excessive computational requirements. Thus, alternative numerical formulations are sought that will allow accurate solutions with reasonable computational effort.

Two general classes of approximations can be identified from the literature on modeling advection-dominated transport. The first is referred to herein as the class of optimal spatial methods, while the second is referred to as the class of characteristic methods. Optimal spatial methods (OSM's) employ an Eulerian approach that is rooted in a minimization of error in the approximation of the spatial derivatives. For example, in the pioneering work of Allen and Southwell[1], a finite difference approximation was developed for the advection and diffusion terms that gives exact nodal values for the simplified case of one-dimensional, steady state, constant coefficient advective-diffusive transport without sources, sinks, or reaction terms. This philosophy has persisted in many other aproximations, including the finite element methods of Christie, *et al.*[14], Hughes and coworkers[32–35,46], Carey[9], Barrett and Morton[2], Demkowitcz and Oden[18], Hemker[24], and Celia *et al.*[11–13]. All of the procedures yield an upstream bias in the resulting approximation. While the theoretical basis for many of these methods is

Paper accepted April 1990. Discussion closes June 1991.

impressive, the approximations tend to be ineffective in transient simulations because of the strong influence of the time derivative. The salient features of this class of approximations may be summarized as follows: (*i*) time truncation error dominates the solutions (*ii*) solutions are characterized by significant numerical diffusion and some phase errors (*iii*) the Courant number ($\mathrm{Cu} \equiv V\Delta t/\Delta x$) is generally restricted to be less than one, and sometimes much less than one. A general comparison of some of these methods is provided by Bouloutas and Celia[5].

Other Eulerian methods can be developed that perform significantly better than OSM approximations. These methods attempt to use a nonzero spatial truncation error (thereby differing from OSM's) to cancel temporal errors and thereby reduce the overall truncation error. The cubic Petrov-Galerkin method of Bouloutas and Celia[6] and the general $N+2$ methods of Westerink and coworkers[8,48] are examples of such procedures. While improved accuracy results from these formulations, they still suffer from strict Courant number limitations.

Because of the hyperbolic nature of advective transport, it is natural to look to characteristic analysis to aid in solving the problem. This philosophy has led to many related approximation techniques, which are called by a variety of names, including Eulerian-Lagrangian methods (ELM)[3,37–39], transport diffusion method[4,31,42], method of characteristics (MOC)[40], modified method of characteristics (MMOC)[19,23,44], and operator splitting methods[15,21,49]. These will be grouped herein under the title of characteristic methods (CM's). Each of these methods has in common the fact that the advective component is treated by a characteristic tracking algorithm (a Lagrangian frame of reference), and the diffusive step is treated separately using a more standard (Eulerian) spatial approximation. These methods have the significant advantage that Courant number restrictions of purely Eulerian methods are alleviated because of the Lagrangian nature of the advection step. Furthermore, because the spatial and temporal dimensions are coupled through the characteristic tracking, the influence of time truncation error present in OSM approximations is greatly reduced.

This paper and a companion one[30] provide a generalization of characteristic methods using an approach that we refer to as a localized adjoint method (LAM). The present paper begins by reviewing the LAM procedure, including discussion of the general approach as well as specific formulations that have been developed to date. This is followed by the specific space-time LAM formulation that naturally leads to a generalized CM approximation. This approach provides a consistent formulation that does not rely on any operator splitting or equation decomposition. In addition, all relevant boundary terms arise naturally in the formulation, and a systematic and complete treatment of boundary condition implementation is presented. This turns out to have significant implications for the calculation of boundary fluxes. An analysis of global mass conservation then leads to the final ELLAM approximation, which is shown to possess the conservative property. Example calculations are presented to illustrate the method. Finally, a discussion of several additional topics is presented, including extension to multiple dimensions, development of higher order methods, formulations for reactive transport equations, and treatment of nonconstant coefficients. The companion paper dwells more thoroughly on the associated theoretical questions.

2. LOCALIZED ADJOINT METHODS

The general approach of localized adjoint methods (LAMs) is based on the philosophy of the algebraic theory of numerical methods presented by Herrera[10,25–29]. In LAM, a weight or test function, call it $w_k(\mathbf{w})$, is used to write a weak form of the governing differential equation of interest. Let the governing differential operator be denoted symbolically by $\mathfrak{L}$, with the governing equation written as

$$\mathfrak{L}u(\mathbf{x}) = f(\mathbf{x}), \quad \mathbf{x} \in \Omega, \tag{1}$$

where u is the dependent variable and $\mathbf{x}$ is the vector of independent variables. The weak form of equation (1) is written as

$$\int_\Omega (\mathfrak{L}u) w_k(\mathbf{x}) \mathrm{d}x = \int_\Omega f(\mathbf{x}) w_k(\mathbf{x}) \mathrm{d}x. \tag{2}$$

In the general LAM approach, the domain Ω is discretized into a number of subintervals or elements $\Omega_e (e = 1, 2, \ldots, E)$. Equation (2) is then written as a sum of elemental boundary integrals and integrals over the interior of each element. Depending on the continuity of u and w_k, this may be done using simple integration-by-parts, using the theory of distributions, or using the general Green's formulas of Ref. 26. This point is discussed in detail in the companion paper[30]. The resulting interior integrals involve an integrand that includes the adjoint of $\mathfrak{L}$ acting on w_k, $\mathfrak{L}^* w_k$. The LAM procedure then defines as test functions those which satisfy the homogeneous adjoint equation within each element, so that $\mathfrak{L}^* w_k = 0$. Therefore all interior elemental integrals are eliminated and only boundary integrals remain to be evaluated. Evaluation of these boundary terms leads to the algebraic approximation of interest. The key to LAM algorithms is the choice of subintervals $\{\Omega_e\}$ and the definition of test functions that locally satisfy the homogeneous adjoint operator. This latter point implies that the test functions vary as the operator varies. In this way, the test functions reflect the physics inherent in the governing equation.

LAM approximations have been applied to ordinary differential equations[10,28,29] and to the spatial dimensions of partial differential equations[11–13]. For ordinary differential equations, optimal approximations can be obtained in the sense that exact nodal values are achieved for the case of constant coefficients and approximations of an arbitrarily high order can be achieved for the case of variable coefficients. These results apply for arbitrary forcing functions and arbitrary boundary conditions. Partial differential equations in multiple spatial dimensions have been solved by forming tensor product test functions[11]. For transient partial differential equations, the LAM approach has been applied in space to achieve a semi-discretization for the linear advection-diffusion equation[12] as well as nonlinear advection-diffusion-reaction systems of transport equations[13]. Standard time-marching algorithms were then used to solve the semi-discrete system. When applied to the advection-diffusion equation, the semi-discrete LAM forms an optimal spatial method. This method therefore suffers from the limitations of all optimal spatial methods, as described in the previous section. However, there is no reason for the LAM approach to be restricted to semi-discrete formulations. Because the LAM approach is quite general, LAM approximations can be applied to the full space-time operator. The next section develops a space-time LAM algorithm that produces a general characteristic method algorithm.

3. AN EULERIAN-LAGRANGIAN LAM FOR ADVECTION-DIFFUSION TRANSPORT EQUATIONS

Consider the one-dimensional transient advection-diffusion equation subject to appropriate initial and boundary conditions,

$$\mathcal{L}u \equiv \frac{\partial u}{\partial t} + V\frac{\partial u}{\partial x} - D\frac{\partial^2 u}{\partial x^2} = f(x, t),$$
$$\begin{aligned} & x \in \Omega_x = [0, l] \\ & t \in \Omega_t = [0, \infty] \text{ ,} \\ & (x, t) \in \Omega_{x,t} \equiv \Omega_x \times \Omega_t, \\ & u(x, 0) = u_I(x) \\ & u(0, t) = u_0(t) \\ & \frac{\partial u}{\partial x}(l, t) = q_l(t). \end{aligned} \tag{3}$$

First- and second-type boundary conditions are chosen for demonstration purposes only; the following development accommodates any combination of boundary conditions. The adjoint operator associated with the operator $\mathcal{L}$ of equation (3) is

$$\mathcal{L}^*w = \frac{\partial w}{\partial t} - V\frac{\partial w}{\partial x} - D\frac{\partial^2 w}{\partial x^2}. \tag{4}$$

The LAM approach is initiated by writing the weak form of equation (3). Let $w(x, t)$ refer to a test function (whose precise form will be determined as part of the LAM development), so that the weak form of equation (3) is

$$\int_0^\infty \int_0^l (\mathcal{L}u - f)w(x, t)\mathrm{d}x\,\mathrm{d}t = 0. \tag{5}$$

As discussed in the previous section, the test function $w(x, t)$ is chosen from the solution space of the homogeneous adjoint equation. In this case, the homogeneous adjoint equation is

$$\mathcal{L}^*w = -\frac{\partial w}{\partial t} - V\frac{\partial w}{\partial x} - D\frac{\partial^2 w}{\partial x^2} = 0. \tag{6}$$

As opposed to the simple developments for ordinary differential operators, the solution space of the partial differential equation (6) is infinite-dimensional. Because the objective of the numerical procedure is derivation of a finite number of algebraic equations, only a finite number of test functions should be chosen. Different choices of test functions (solutions of equation (6)) lead to different classes of approximations, including families of optimal spatial methods and general characteristics methods.

By analogy to the tensor product approach of Celia *et al.*[11], a product solution of the form $w(x, t) = \xi(x)\tau(t)$ could be sought such that $\xi(x)$ satisfies the homogeneous spatial operator of equation (6) while $\tau(t)$ satisfies the temporal part. Such a space-time split, defined on a rectangular discretization of $\Omega_{x,t}$, leads to optimal spatial algorithms involving exponential weightings in space. The result is analogous to the semi-discretizations presented by Celia *et al.*[12,13].

To derive a general family of characteristic methods (CM's), a different set of solutions to equation (6) must be used. In particular, consider solutions to equation (6) which satisfy the two homogeneous sub-equations that are grouped based on common order of derivatives, viz. $(\partial w/\partial t) + V(\partial w/\partial x) = 0$ and $D(\partial^2 w/\partial x^2) = 0$. The second constraint implies linear functions of x, while the first constraint implies w = constant along lines $x - x_0 = V(t - t_0)$. A natural choice for such a test function can be defined with respect to a rectangular array of nodes in space-time as follows,

$$w_i^{n+1}(x, t) = \begin{cases} \dfrac{x - x_{i-1}}{\Delta x} + V\dfrac{t^{n+1} - t}{\Delta x}, & (x, t) \in \Omega_1^i, \\ \dfrac{x_{i+1} - x}{\Delta x} - V\dfrac{t^{n+1} - t}{\Delta x}, & (x, t) \in \Omega_2^i, \\ 0, & \text{all other } (x, t), \end{cases} \tag{7}$$

where subscript i denotes spatial location ($x_i \equiv i(\Delta x)$ for constant spatial step Δx), superscript n denotes time level ($t^n \equiv n(\Delta t)$ for constant time step Δt), and the test function $w_i^{n+1}(x, t)$ is associated with spatial location i and temporal location $n + 1$. In writing equation (7), constant node spacing Δx has been assumed. The regions Ω_1^i and Ω_2^i are illustrated in Fig. 1, as is a typical test function. The function $w_i^{n+1}(x, t)$ has the properties that it is

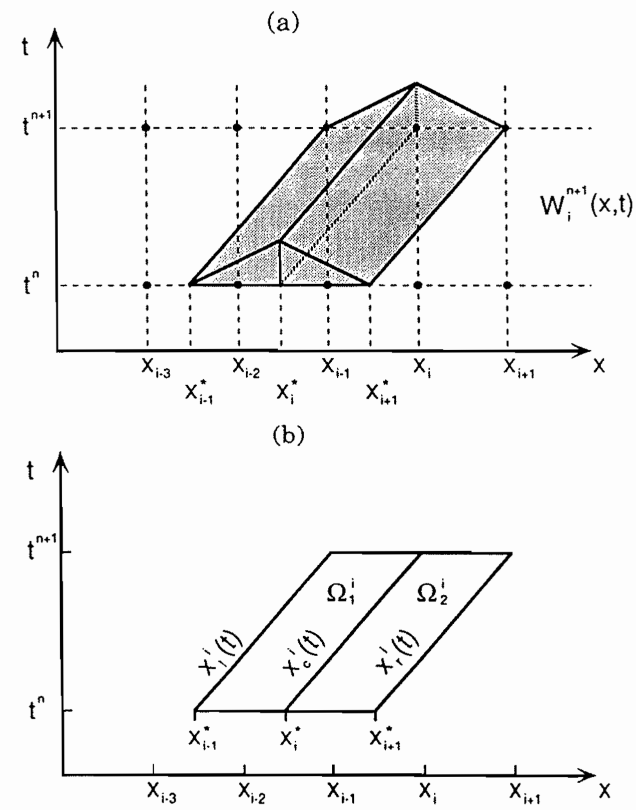

Fig. 1. (a) General interior test function $w_i^{n+1}(x, t)$, and (b) associated geometric definitions

$\mathbb{C}^0[\Omega_x]$, $\mathbb{C}^{-1}[\Omega_t]$, is nonzero over only one time step (t^n to t^{n+1}) with discontinuities aligned along t^n and t^{n+1}, and the lines of spatial derivative discontinuities align with the characteristics that intersect the nodes x_{i-1}, x_i, and x_{i+1} at time level t^{n+1}.

Given this test function definition, the weak form of the equation can be evaluated by standard integration procedures. Let the spatial locations at time level t^n that are on the characteristic curves that intersect points x_{i-1}, x_i, x_{i+1} at t^{n+1} be denoted as x^*_{i-1}, x^*_i, and x^*_{i+1}, respectively, as illustrated in Fig. 1. These points are often referred to as the 'foot of the characteristic' points. In addition, let the characteristic curves that pass through points x_{i-1}, x_i, and x_{i+1} at time t^{n+1} be identified by $x^i_l(t)$, $x^i_c(t)$, and $x^i_r(t)$, respectively, as illustrated in Fig. 1. The weak form of equation (3) can be rewritten in an equivalent form by applying integration by parts. If $u(x, t)$ is assumed to be at least $\mathbb{C}^1$-continuous in x and $\mathbb{C}^0$-continuous in t (cases of less restrictive continuity are treated in the companion paper[30]), then the integrations of equation (5) can be written equivalently as a sum of elemental integrals. Integration by parts can then be applied element-by-element, where 'elements' are defined as the regions Ω^i_1, Ω^i_2, etc. Evaluation of the weak form (5), with $w^{n+1}_i(x, t)$ used as the test function, leads to the following expression.

$$\int_0^\infty \int_0^l (\mathcal{L}u - f) w_i^{n+1}(x, t)\,dx\,dt = 0$$

$$= \int_0^\infty \int_0^l \left[\frac{\partial u}{\partial t} + V\frac{\partial u}{\partial x} - D\frac{\partial^2 u}{\partial x^2} - f(x, t) \right] w_i^{n+1}(x, t)\,dx\,dt$$

$$= \int_{x_{i-1}}^{x_{i+1}} u(x, t^{n+1}) w_i^{n+1}(x, t^{n+1})\,dx$$

$$- \int_{x^*_{i-1}}^{x^*_{i+1}} u(x, t^n) w_i^{n+1}(x, t^n)\,dx$$

$$- D\left[\int_{t^n}^{t^{n+1}} u(x^i_l(t), t) \left[\!\left[\frac{\partial w_i^{n+1}}{\partial x} \right]\!\right]_{x^i_l(t)} dt \right.$$

$$+ \int_{t^n}^{t^{n+1}} u(x^i_c(t), t) \left[\!\left[\frac{\partial w_i^{n+1}}{\partial x} \right]\!\right]_{x^i_c(t)} dt$$

$$\left. + \int_{t^n}^{t^{n+1}} u(x^i_r(t), t) \left[\!\left[\frac{\partial w_i^{n+1}}{\partial x} \right]\!\right]_{x^i_r(t)} dt \right]$$

$$+ \int_{\Omega^i_1} u(x, t) \mathcal{L}^* w_i^{n+1}\,dx\,dt$$

$$+ \int_{\Omega^i_2} u(x, t) \mathcal{L}^* w_i^{n+1}\,dx\,dt$$

$$- \int_{\Omega^i_1 \cup \Omega^i_2} f(x, t) w_i^{n+1}(x, t)\,dx\,dt = 0, \tag{8}$$

where the double bracket notation denotes a spatial jump operator, $[\![\cdot]\!]_{x_k} \equiv \lim_{\epsilon\to 0}[(\cdot)_{x_k+\epsilon} - (\cdot)_{x_k-\epsilon}]$. Due to the special choice of test function given by equation (7), $\mathcal{L}^* w_i^{n+1} = 0$ in both Ω^i_1 and Ω^i_2, so that the interior integrals involving $u(x, t)$ are eliminated. Furthermore, the spatial jump operators can be evaluated explicitly from equation (7) as

$$\left[\!\left[\frac{\partial w_i^{n+1}}{\partial x} \right]\!\right]_{x^i_l(t)} = \left[\!\left[\frac{\partial w_i^{n+1}}{\partial x} \right]\!\right]_{x^i_r(t)} = \frac{1}{\Delta x},$$

$$\left[\!\left[\frac{\partial w_i^{n+1}}{\partial x} \right]\!\right]_{x^i_c(t)} = \frac{-2}{\Delta x}.$$

Equation (8) can therefore be simplified as

$$\int_{x_{i-1}}^{x_{i+1}} u(x, t^{n+1}) w_i^{n+1}(x, t^{n+1})\,dx$$

$$- \int_{x^*_{i-1}}^{x^*_{i+1}} u(x, t^n) w_i^{n+1}(x, t^n)\,dx$$

$$- D\left[\left(\frac{1}{\Delta x}\right) \int_{t^n}^{t^{n+1}} u(x^i_l(t), t)\,dt \right.$$

$$- \left(\frac{2}{\Delta x}\right) \int_{t^n}^{t^{n+1}} u(x^i_c(t), t)\,dt$$

$$\left. + \left(\frac{1}{\Delta x}\right) \int_{t^n}^{t^{n+1}} u(x^i_r(t), t)\,dt \right]$$

$$= \int_{\Omega^i_1 \cup \Omega^i_2} f(x, t) w_i^{n+1}(x, t)\,dx\,dt. \tag{9}$$

Equations (7) through (9) have been written under the assumptions of constant node spacing Δx and constant coefficients in the governing equation, and for characteristics that do not intersect the spatial boundaries. For nonconstant spacing, the test functions change as follows:

$$w_i^{n+1}(x, t) = \begin{cases} \dfrac{x - x_{i-1}}{\nabla x_i} + V\dfrac{t^{n+1} - t}{\nabla x_i}, & (x, t) \in \Omega^i_1, \\[2ex] \dfrac{x_{i+1} - x}{\Delta x_i} - V\dfrac{t^{n+1} - t}{\Delta x_i}, & (x, t) \in \Omega^i_2 \\[2ex] 0, & \text{all other } (x, t), \end{cases} \tag{10}$$

where $\nabla x_i \equiv x_i - x_{i-1}$ and $\Delta x_i \equiv x_{i+1} - x_i$ are the usual backward and forward difference operators. This modification does not change equation (8), and equation (9) is modified only by a revised determination of the locations x^*_{i-1}, x^*_i x^*_{i+1}, and by the evaluation of spatial jumps, which are now

$$\left[\!\left[\frac{\partial w_i^{n+1}}{\partial x} \right]\!\right]_{x^i_l(t)} = \frac{1}{\nabla x_i}, \quad \left[\!\left[\frac{\partial w_i^{n+1}}{\partial x} \right]\!\right]_{x^i_r(t)} = \frac{1}{\Delta x_i},$$

$$\left[\!\left[\frac{\partial w_i^{n+1}}{\partial x} \right]\!\right]_{x^i_c(t)} = \left(\frac{1}{\nabla x_i} + \frac{1}{\Delta x_i} \right)$$

When the velocity coefficient in the governing equation is not constant, the characteristics are, in general, not parallel. The definition of the test function then must be modified to reflect this fact. This case is discussed in some detail in Section 8 of this paper. One possibility for this case is to assume that the locations of characteristic lines between the characteristics that pass through adjacent nodes at t^{n+1} are determined by linear interpolation in space for all $t^n \le t \le t^{n+1}$. Then the appropriate test function is

$$w_i^{n+1}(x, t) = \begin{cases} \dfrac{x - x_{i-1}}{x_c^i(t) - x_l^i(t)} + V\dfrac{t^{n+1} - t}{x_c^i(t) - x_l^i(t)}, & (x, t) \in \Omega_1^i, \\ \dfrac{x_{i+1} - x}{x_r^i(t) - x_c^i(t)} - V\dfrac{t^{n+1} - t}{x_r^i(t) - x_c^i(t)}, & (x, t) \in \Omega_2^i \\ 0, & \text{all other } (x, t). \end{cases} \quad (11)$$

For this case, the only change in the resulting numerical approximation is again in the location of the feet of the characteristics and in the spatial jumps. Now the jumps are functions of time, viz.,

$$\left[\!\left[\frac{\partial w_i^{n+1}}{\partial x}\right]\!\right]_{x_l^i(t)} = \frac{1}{x_c^i(t) - x_l^i(t)},$$

$$\left[\!\left[\frac{\partial w_i^{n+1}}{\partial x}\right]\!\right]_{x_r^i(t)} = \frac{1}{x_r^i(t) - x_c^i(t)},$$

$$\left[\!\left[\frac{\partial w_i^{n+1}}{\partial x}\right]\!\right]_{x_c^i(t)} = -\left[\frac{1}{x_c^i(t) - x_l^i(t)} + \frac{1}{x_r^i(t) - x_c^i(t)}\right]$$

Because these terms are functions of time, they cannot be removed from the integrations of equation (8). The resulting approximation is thus of the form

$$\begin{aligned} &\int_{x_{i-1}}^{x_{i+1}} u(x, t^{n+1}) w_i^{n+1}(x, t^{n+1})\,dx \\ &- \int_{x_{i-1}^*}^{x_{i+1}^*} u(x, t^n) w_i^{n+1}(x, t^n)\,dx \\ &-D\left[\int_{t^n}^{t^{n+1}} \left[\frac{1}{x_c^i(t) - x_l^i(t)}\right] u(x_l^i(t), t)\,dt\right. \\ &- \int_{t^n}^{t^{n+1}} \left[\frac{1}{x_c^i(t) - x_l^i(t)} + \frac{1}{x_r^i(t) - x_c^i(t)}\right] u(x_c^i(t), t)\,dt \\ &\left.+ \int_{t^n}^{t^{n+1}} \left[\frac{1}{x_r^i(t) - x_c^i(t)}\right] u(x_r^i(t), t)\,dt\right] \\ &= \int_{\Omega_1^i \cup \Omega_2^i} f w_i^{n+1}\,dx\,dt. \end{aligned} \quad (12)$$

In the developments that follow, V and Δx are held constant. This allows the general ideas of the method to be demonstrated clearly.

Because of the special test functions chosen, this class of LAM is referred to as an Eulerian-Lagrangian LAM (ELLAM). Notice that the unknown function $u(x, t)$ has not yet been approximated by any specific functional form. The integrals that appear in this equation may in fact be approximated in many different ways. Different approximations of these integrals lead to different CM algorithms reported in the literature. In all of these, the integrals are approximated in terms of nodal values of u at the discrete time levels t^n and t^{n+1}, so that the unknowns in the equation ultimately include the nodal values at time t^{n+1}, $\{U_0^{n+1}, U_1^{n+1}, \ldots, U_E^{n+1}\}$, where U_i^{n+1} is an approximation to $u(x_i, t^{n+1})$. For example, piecewise linear spatial interpolation of u at time levels t^{n+1} and t^n, coupled with a one-point (at $t = t^{n+1}$) fully implicit approximation to the temporal integrals, leads to the modified method of characteristics (MMOC) of Douglas and Russell[19] and others. Given the definition of the test function $w_i^{n+1}(x, t)$, and the assumptions of constant Δx and V, the resulting discrete approximation is

$$\begin{aligned} &\left(\frac{\Delta x}{6}\right) U_{i+1}^{n+1} + \left(\frac{2\Delta x}{3}\right) U_i^{n+1} + \left(\frac{\Delta x}{6}\right) U_{i+1}^{n+1} \\ &-(\Delta x)\left[\beta_1 U_{i-Nc-2}^n + \beta_2 U_{i-Nc-1}^n\right. \\ &\left.+\beta_3 U_{i-Nc}^n + \beta_4 U_{i-Nc+1}^n\right] \\ &- \frac{D(\Delta t)}{\Delta x}\left[U_{i+1}^{n+1} - 2U_i^{n+1} + U_{i+1}^{n+1}\right] = F_i^{n+1}, \end{aligned} \quad (13)$$

where Nc is the (truncated) integer value of the Courant number Cu

$$\mathrm{Cu} \equiv \frac{V\Delta t}{\Delta x}, \quad \alpha \equiv 1 - [\mathrm{CU{-}Nc}],$$

$$\beta_1 = \frac{1}{6} - \frac{\alpha}{2} + \frac{\alpha^2}{2} - \frac{\alpha^3}{6},$$

$$\beta_2 = \frac{2}{3} - \alpha^2 + \frac{\alpha^3}{2},$$

$$\beta_3 = \frac{1}{6} + \frac{\alpha}{2} + \frac{\alpha^2}{2} - \frac{\alpha^3}{2},$$

and

$$\beta_4 = \frac{\alpha^3}{6}.$$

The grouping of terms involving β_i corresponds to exact evaluation of the integral at $t = t^n$, namely

$$\int_{x_{i-1}^*}^{x_{i+1}^*} u(x, t^n) w_i^{n+1}(x, t^n)\,dx,$$

using piecewise linear interpolation for $u(x, t^n)$ and assuming constant Δx. The usual MMOC approach approximates this term using numerical integration, which is the most practical option for nonconstant grid spacing and/or nonconstant velocity fields. The exact integration is used here for demonstration purposes only, and to indicate that it is a reasonable option when both Δx and V are constant. Baptista[3] has compared a variety of interpolation schemes for the integrals at time t^n in the context of Eulerian-Lagrangian Methods. These procedures are closely related to MMOC and are again a subset of the general CM equations that result from ELLAM.

Traditional MMOC and ELM algorithms have a substantial base of theoretical results[17,19,23,44] and computational experience[3,37–39,45]. However, several problems remain unresolved. Chief among them are treatment of boundary conditions and evaluation of spatial integrals along $t = t^n$. Significant experience has been gained in integral evaluation (see, for example, Ref. 3). However, as discussed by Russell[43], boundary conditions have usually been dealt with in *ad hoc* ways. When a characteristic line passing through points x_{i-1}, x_i, or x_{i+1} at time t^{n+1} crosses the boundary between times t^n and t^{n+1}, call it time t^*, the boundary information must be incorporated into the approximating equation. Dirichlet conditions are easiest to deal with, although most algorithms fail to accommodate the reduced time interval $t^{n+1} - t^*$ associated with certain boundary terms (see Section 4). Flux boundary conditions are usually ignored, although some developments appear in the literature (e.g., Ref. 38). Based on the treatment of boundary conditions, all MMOC and ELM approximations proposed in the literature appear to be inherently non-mass-conservative. In variable-velocity flow fields, failure to conserve mass also results from inexact representations of the characteristics.

The ELLAM approach outlined above overcomes the boundary condition and mass conservation problems inherent in other CM approaches. As the next section demonstrates, the ELLAM approach provides a systematic and consistent methodology for proper incorporation of boundary conditions. Correct treatment of boundary conditions leads to an overall approximation that can be shown to possess the conservative property, thereby assuring conservation of mass in the numerical solution. Therefore, while ELLAM provides a general framework from which many traditional ELM and MMOC approximations can be derived, it also provides important additions to the methods by properly incorporating boundary information and by possessing demonstrable mass conservation. In Section 8, conservation in the case of approximate characteristics dictated by variable velocity fields will be discussed.

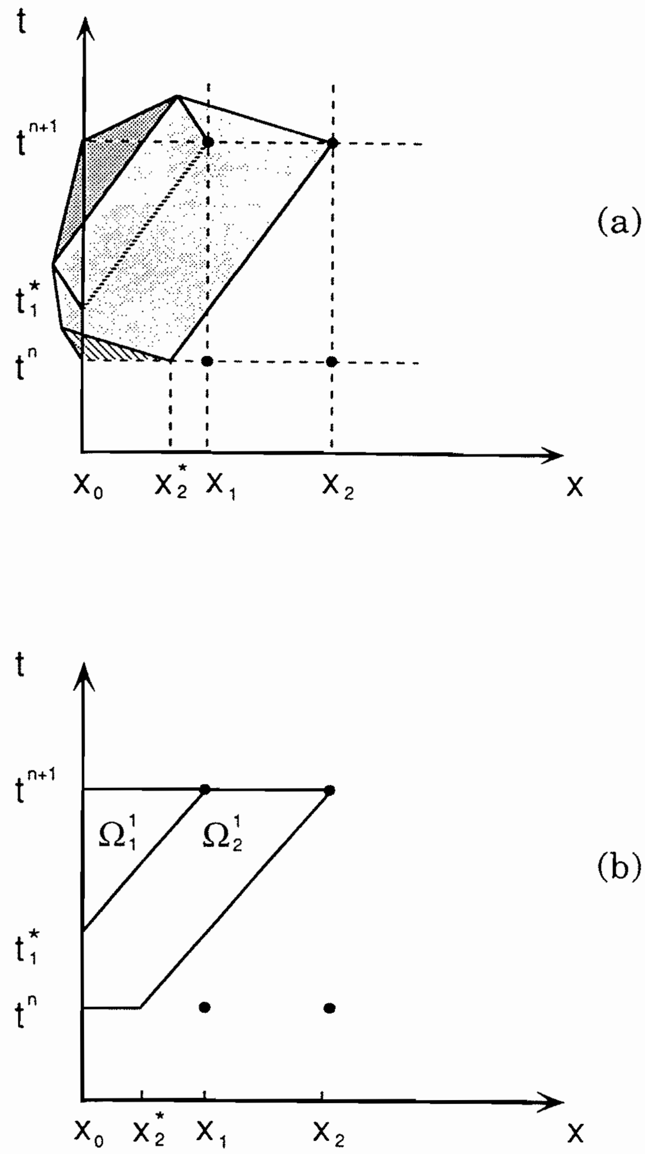

Fig. 2. (a) Test function $w_l^{n+1}(x, t)$, and (b) associated geometric definitions

4. IMPLEMENTATION OF BOUNDARY CONDITIONS

The general CM equation (12) must be modified when one or more of the characteristic curves $x_l^i(t)$, $x_c^i(t)$, $x_r^i(t)$ intersects the spatial boundary. When this occurs, boundary conditions are introduced into the approximating equations. Proper evaluation of the weak form (8) inherently accommodates all relevant boundary information, and provides for proper incorporation of boundary conditions at all boundaries. As the following derivation demonstrates, careful treatment of both inflow and outflow boundaries allows proper incorporation of boundary conditions and provides a formulation that demonstrably conserves global mass. In addition, the ELLAM equations apply to both the advection-diffusion ($D \neq 0$) and pure advection ($D = 0$) cases with no modification of the equations required as $D \to 0$.

To demonstrate the incorporation of boundary conditions at the inflow boundary ($x = x_0 = 0$ for the example of equation (3) with $V > 0$), let us consider an example for which the Courant number $\mathrm{Cu} \equiv [V(\Delta t)/(\Delta x)]$ is between 1 and 2. The general case of arbitrary Cu is treated in the appendix. For the case of $1 \leq \mathrm{Cu} < 2$, the characteristic curve that passes through node 1 ($x = x_1$) at time t^{n+1} intersects the boundary at $x = x_0 = 0$ at time $t_1^* \geq t^n$. Therefore, equations that involve this characteristic will be influenced by boundary conditions. Consider the ELLAM equation associated with node 1. The test function $w_1^{n+1}(x, t)$, illustrated in Fig. 2, differs from the general function w_i^{n+1} of Fig. 1 because part of w_1^{n+1} intersects the boundary at $x = 0$ with nonzero value. Therefore, evaluation of the general ELLAM equation (7) is modified by boundary influences. The ELLAM equation associated with $w_1^{n+1}(x, t)$ is derived in the same way as equations (8) and (9): elemental integration by parts is applied to each term, the condition that $\mathcal{L}^* w_1^{n+1} = 0$ in each element is recognized, and the appropriate jumps in the spatial derivative $[\![(\partial w/\partial x)]\!]$ are evaluated to produce

$$\int_{x_0}^{x_2} u(x, t^{n+1}) w_1^{n+1}(x, t^{n+1})\, dx$$

$$- \left[\int_{x_0}^{x_2^*} u(x, t^n) w_1^{n+1}(x, t^n)\, dx \right.$$

$$\left. + V \int_{t^n}^{t^{n+1}} u(0, t) w_1^{n+1}(0, t)\, dt \right]$$

$$- D \left[\left(\frac{1}{\Delta x}\right) \int_{t_l^*}^{t^{n+1}} u(0, t)\, dt \right.$$

$$- \left(\frac{2}{\Delta x}\right) \int_{t_l^*}^{t^{n+1}} u(x_c^1(t), t)\, dt$$

$$\left. + \left(\frac{1}{\Delta x}\right) \int_{t^n}^{t^{n+1}} u(x_r^1(t), t)\, dt \right]$$

$$+ D \int_{t^n}^{t^{n+1}} \frac{\partial u}{\partial x}(0, t) w_1^{n+1}(0, t)\, dt$$

$$+ D \left(\frac{1}{\Delta x}\right) \int_{t^n}^{t_l^*} u(0, t)\, dt$$

$$= \int_{\Omega_1^1 \cup \Omega_2^1} f(x, t) w_1^{n+1}(x, t)\, dx\, dt. \qquad (14)$$

Examination of equation (14) indicates that the spatial integration at time t^n is modified by the boundary at $x = 0$. While this integration spans a distance of $2\Delta x$ in equation (7), it spans $(2 - \mathrm{Cu})\Delta x$ in equation (14). The part that is cut off by the boundary, corresponding to the distance $\mathrm{Cu}(\Delta x)$, is picked up by the third integral on the left side of equation (14), which involves the boundary value $u(0, t)$. The next three integrals in equation (14) correspond to the three diffusive terms in equation (7), except that the left integral is evaluated along $x = 0$ and the integrand is the boundary value $u(0, t)$. Finally, the last two integrals on the left side of equation (14) are again integrals that are evaluated along the boundary $x = 0$: the second of these involves the function $u(0, t)$ but the first involves the spatial gradient $(\partial u/\partial x)(0, t)$. Notice that this latter integral introduces an additional degree of freedom at the boundary, so that both $u(0, t)$ and $(\partial u/\partial x)(0, t)$ are present in this equation. Even when a first type boundary condition is specified at $x = 0$, the flux at the boundary may need to be determined due to the presence of this integral. Therefore, an additional equation should be written, that which corresponds to node 0, with test function $w_0^{n+1}(x, t)$ (see Fig. 3). This is in contrast to standard finite element methods, wherein the boundary flux need not be explicitly determined when first type boundary conditions are prescribed. The reason that both boundary values appear in the ELLAM formulation is that the space-time LAM elements of Fig. 1 are not parallel to the time axis, while standard semidiscrete finite elements correspond to rectangular space-time elements with sides parallel to the space-time coordinate axes.

Similar terms arise in all equations for which the test function is nonzero along a portion of the spatial boundary. As illustrated in the development for arbitrary Courant number presented in the appendix, equations associated with all nodes to the left of node $Nc + 2$ will have contributions from the inflow boundary (assuming constant Δx and V), where Nc is the (truncated) integer value of the Courant number Cu. For the present case of $1 \leq \mathrm{Cu} < 2$, $Nc = 1$ and equations associated with w_0^{n+1}, w_1^{n+1}, and w_2^{n+1} will have boundary contributions. The relevant ELLAM equations for w_0^{n+1} and w_2^{n+1} are, respectively,

$$\int_{x_0}^{x_1} u(x, t^{n+1}) w_0^{n+1}(x, t^{n+1})\, dx$$

$$- V \int_{t_l^*}^{t^{n+1}} u(0, t) w_0^{n+1}(0, t)\, dt$$

$$- D \left[\left(\frac{-1}{\Delta x}\right) \int_{t_l^*}^{t^{n+1}} u(0, t)\, dt \right.$$

$$\left. + \left(\frac{1}{\Delta x}\right) \int_{t_l^*}^{t^{n+1}} u(x_r^0(t), t)\, dt \right]$$

$$+ D \int_{t_l^*}^{t^{n+1}} \frac{\partial u}{\partial x}(0, t) w_0^{n+1}(0, t)\, dt$$

$$= \int_{\Omega_2^0} f w_0^{n+1}\, dx\, dt \qquad (15a)$$

and,

$$\int_{x_1}^{x_3} u(x, t^{n+1}) w_2^{n+1}(x, t^{n+1})\, dx$$

$$- \left[\int_{x_0}^{x_3^*} u(x, t^n) w_2^{n+1}(x, t^n)\, dx \right.$$

$$\left. + V \int_{t^n}^{t_l^*} u(0, t) w_2^{n+1}(0, t)\, dt \right]$$

$$- D \left[\left(\frac{1}{\Delta x}\right) \int_{t_l^*}^{t^{n+1}} u(x_l^2(t), t)\, dt \right.$$

$$- \left(\frac{2}{\Delta x}\right) \int_{t^n}^{t^{n+1}} u(x_c^2(t), t)\, dt$$

$$\left. + \left(\frac{1}{\Delta x}\right) \int_{t^n}^{t^{n+1}} u(x_r^2(t), t)\, dt \right]$$

$$+ D \int_{t^n}^{t_l^*} \frac{\partial u}{\partial x}(0, t) w_2^{n+1}(0, t)\, dt$$

$$- D \left(\frac{1}{\Delta x}\right) \int_{t^n}^{t_l^*} u(0, t)\, dt$$

$$= \int_{\Omega_2^1 \cup \Omega_1^2} f w_2^{n+1}\, dx\, dt. \qquad (15b)$$

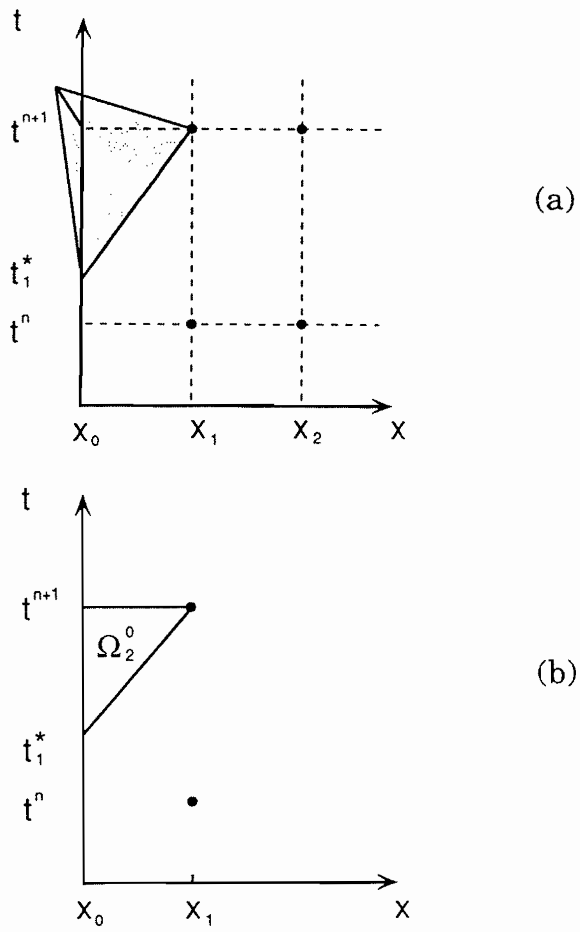

Fig. 3. (a) Test function $w_0^{n+1}(x, t)$, and (b) associated geometric definitions

Equations (14), (15a), and (15b) are the three equations (for $Nc = 1$) in which inflow boundary conditions appear. If a first-type boundary condition is specified, then all integrals involving $u(0, t)$ are known and the integrals involving the diffusive flux $D(\partial u/\partial x)(0, t)$ are unknown. Conversely, for a second-type boundary condition, $(\partial u/\partial x)(0,t)$ is known and $u(0, t)$ must be determined. Finally, for a third-type boundary conditions, the gradient $(\partial u/\partial x)(0, t)$ may be written in terms of $u(0, t)$, or vice versa. For all three scenarios, both u and $(\partial u/\partial x)$ must be determined at the inflow boundary, and equation (15a) is therefore required. Notice that in all three equations ((14), (15a), (15b)) the advective and diffusive fluxes may be combined: in equation (15a), for example, the total boundary flux term is

$$-\int_{t_1^*}^{t^{n+1}} \left[Vu(0, t) - D\frac{\partial u}{\partial x}(0, t) \right] w_0^{n+1}(0, t)\mathrm{d}t.$$

This is convenient for implementation of third-type boundary conditions and also makes it easier to see that the final set of equations possesses the conservative property (see Section 5). In addition, if a one-point integration rule is used to approximate the boundary integrals, and the integration point is $t = t^{n+1}$, then the flux term in, for example, equation (14),

$$\int_{t^n}^{t^{n+1}} \frac{\partial u}{\partial x}(0, t) w_1^{n+1}(0, t)\mathrm{d}t,$$

is zero because $w_i^{n+1}(0, t^{n+1}) = 0$ for all $i > 0$. Therefore, while this diffusive type of boundary integral is present in all ELLAM equations that have characteristics that intersect the inflow boundary, further approximation of the equations may eliminate this term. This point appears to have significance for the resulting matrix structure, as discussed in Section 5.

Notice that, in general, when a characteristic crosses the boundary, some of the integrals that arise in the ELLAM equations span a time less than Δt. In particular, the integrals related to the diffusion term (for example, the third and fourth integrals in equation (15a)) span the time increment $t^{n+1} - t_1^*$, which is less than Δt. Thus the diffusion part of the equation applies over a reduced time step. This effect, which was unnoticed by most CM references in the literature (an exception being Douglas *et al.*[20]), arises naturally in the ELLAM formulation.

These issues about the one-point integration and time intervals less than Δt are discussed further, from a different point of view, by Russell[43]. There, an equivalent formulation is derived, in which the terms multiplied by D in equations (14), (15a), and (15b) are obtained by integrating the diffusive term in equation (8) by parts once instead of twice. Russell's paper emphasizes the special case of ELLAM with one-point integration as an extension of MMOC.

Treatment of outflow boundary conditions is somewhat more involved. We herein propose an approach that inherently conserves global mass and directly accommodates the case of pure advection ($D = 0$), for which no outflow boundary condition is specified. To begin, let

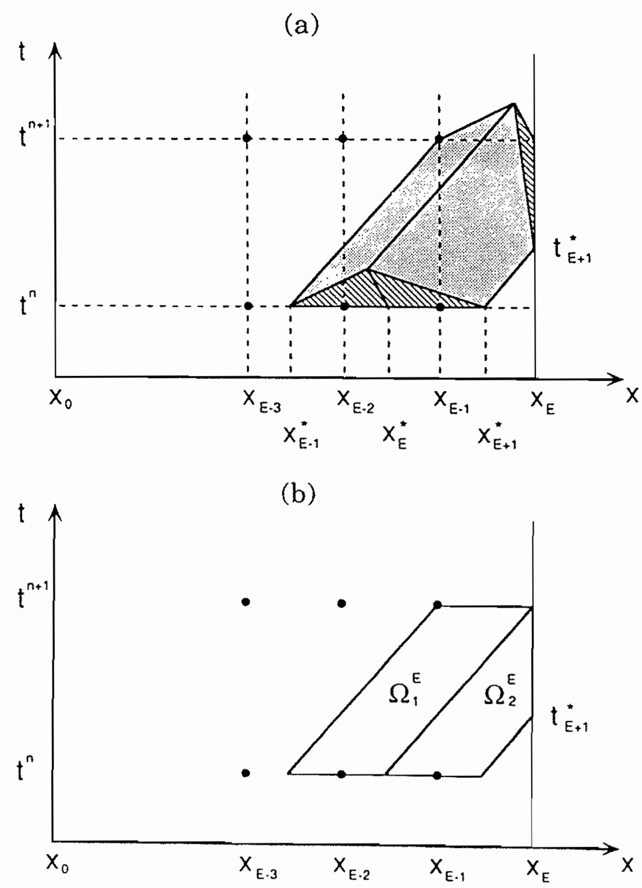

Fig. 4. (a) Test function $w_E^{n+1}(x, t)$, and (b) associated geometric definitions

the boundary condition of equation (3), namely $(\partial u/\partial x)(l, t) = q_l(t)$, pertain. Again, consider the case of $1 \leq Cu < 2$, so that $Nc = 1$. ELLAM equations would be written for nodes $x_0, x_1, x_2, \ldots, x_{E-1}$; equations (14), (15a), and (15b) provide expressions for $i = 0, 1, 2$, respectively, while equation (9) applies for $i = 3, 4, \ldots, E-1$. If the only unknowns in these equations are nodal values at the new time level, then these equations constitute a set of E equations in $E+2$ unknowns (unknowns $(\partial U_0^{n+1}/\partial x), U_0^{n+1}, U_1^{n+1}, U_2^{n+1}, \ldots, U_E^{n+1}$). One additional equation is available from the inflow boundary condition. If a first-type boundary condition were given at $x = l$, then U_E^{n+1} would also be known and, coupled with the boundary condition at $x = 0$, the system could be solved for all nodal unknowns listed above. However, if a second-type boundary condition is prescribed, then U_E^{n+1} is not known and an additional equation must be written, that associated with $w_E^{n+1}(x, t)$. The function $w_E^{n+1}(x, t)$ is illustrated in Fig 4. Notice that this is the first test function that has a nonzero region along $x = x_E = l$, $t^n \leq t \leq t^{n+1}$. Therefore boundary terms at $x = l$ will appear in this equation. Evaluation of the ELLAM equation for w_E^{n+1} leads to the following expression:

$$\int_{x_{E-1}}^{x_E} u(x, t^{n+1})w_E^{n+1}(x, t^{n+1})\,dx + V\left[\int_{t_{E+1}^*}^{t^{n+1}} u(l, t)w_E^{n+1}(l, t)\,dt\right] - \int_{x_{E-1}^*}^{x_{E+1}^*} u(x, t^n)w_E^{n+1}(x, t^n)\,dx$$
$$-D\left[\left(\frac{1}{\Delta x}\right)\int_{t^n}^{t^{n+1}} u(x_l^E(t), t)\,dt - \left(\frac{2}{\Delta x}\right)\int_{t^n}^{t^{n+1}} u(x_c^E(t), t)\,dt + \left(\frac{1}{\Delta x}\right)\int_{t^n}^{t_{E+1}^*} u(x_r^E(t), t)\,dt\right]$$
$$-D\int_{t_{E+1}^*}^{t^{n+1}} \frac{\partial u}{\partial x}(l, t)w_E^{n+1}(l, t)\,dt - D\left(\frac{1}{\Delta x}\right)\int_{t_{E+1}^*}^{t^{n+1}} u(l, t)\,dt$$
$$= \int_{\Omega_1^E \cup \Omega_2^E} f w_E^{n+1}\,dx\,dt. \tag{16}$$

For a second-type boundary condition, $(\partial u/\partial x)(l, t)$ would be prescribed as the outflow boundary condition while $u(l, t)$ is unknown for $t^n < t \leq t^{n+1}$. One possibility for evaluation of $u(l, t)$, $t^n < t \leq t^{n+1}$, is a simple interpolation between U_E^n and U_E^{n+1}. Then, no additional unknown is introduced in equation (16), and the system of equations would be closed. Another option is to place an additional node at the location (x_E, t_{E+1}^*), and to define an additional nodal unknown at this point. For the latter case, let a node be added at location (x_E, t_{E+1}^*), call it node α_1, with the associated discrete unknown denoted by U_{α_1}. Because this adds another unknown to the system, another algebraic equation must be sought. To achieve this, an ELLAM equation can be written for the test function $w_{E+1}^{n+1}(x, t)$, with only that portion of the test function within the domain $\Omega_{x,t}$ used for the approximation (see Fig. 5). Use of $w_{E+1}^{n+1}(x, t)$ as the test function leads to the following ELLAM equation:

$$V\int_{t^n}^{t^{n+1}} u(l, t)w_{E+1}^{n+1}(l, t)\,dt - \int_{x_E^*}^{x_E} u(x, t^n)w_{E+1}^{n+1}(x, t^n)\,dx$$
$$-D\left[\left(\frac{1}{\Delta x}\right)\int_{t^n}^{t^{n+1}} u(x_l^{E+1}(t), t)\,dt - \left(\frac{2}{\Delta x}\right)\int_{t^n}^{t_{E+1}^*} u(x_c^{E+1}(t), t)\,dt\right]$$
$$-D\int_{t^n}^{t^{n+1}} \frac{\partial u}{\partial x}(l, t)w_{E+1}^{n+1}(l, t)\,dt + D\left(\frac{1}{\Delta x}\right)\left[\int_{t_{E+1}^*}^{t^{n+1}} u(l, t)\,dt - \int_{t^n}^{t_{E+1}^*} u(l, t)\,dt\right]$$
$$= \int_{\Omega_1^{E+1} \cup \Omega_2^{E+1}} f w_{E+1}^{n+1}\,dx\,dt. \tag{17}$$

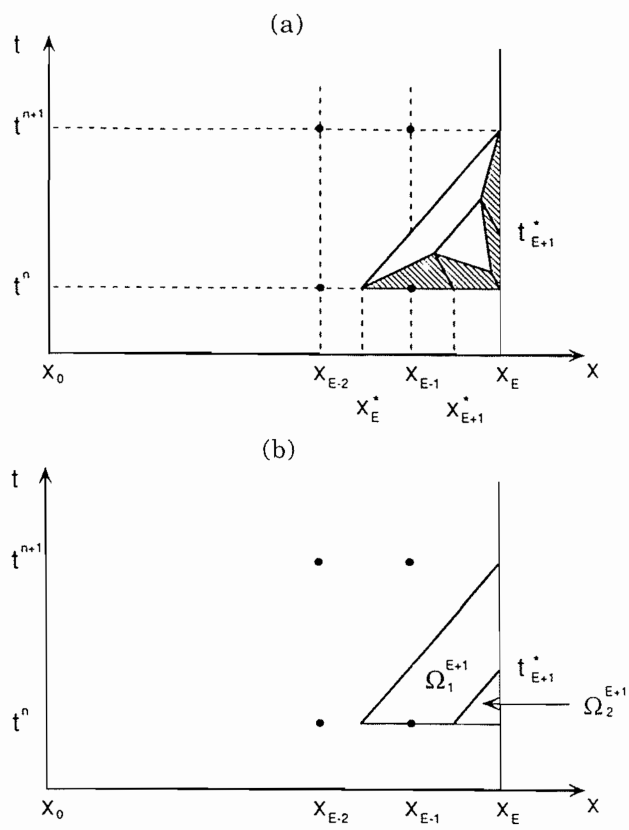

Fig. 5. (a) Test function $w_{E+1}^{n+1}(x, t)$, and (b) associated geometric definitions

Integrals along the boundary $x = x_E = l$ can again be approximated using discrete nodal values. Because $w_{E+1}^{n+1}(l, t)$ is nonzero at $t = t^n$, and all information is assumed known for $t \le t^n$, it is this information at node E and time t^n that effectively serves to close the system. For this case of second-type outflow boundary conditions and $Nc = 1$, there are $E + 2$ ELLAM equations written, corresponding to $w_0^{n+1}, w_1^{n+1}, \ldots, w_{E+1}^{n+1}$. These are solved for the nodal unknowns $(\partial U_0^{n+1}/\partial x)$, U_1^{n+1}, $U_2^{n+1}, \ldots, U_E^{n+1}$, U_{α_1}. The nodal values that are known are U_0^{n+1} (from the inflow boundary condition); $(\partial U_E^{n+1}/\partial x)$, $(\partial U_{\alpha_1}/\partial x)$, and $(\partial U_E^n/\partial x)$ (from the outflow boundary condition); and U_E^n (from the solution at the previous time step).

While these equations provide a solution for the unknowns of interest, they generally fail to conserve global mass. The next section addresses the question of mass conservation and presents a modification to these equations so that the resulting set of ELLAM equations possesses the conservative property.

5. GLOBAL MASS CONSERVATION

This section examines the global mass conservation properties of the ELLAM algorithm. As was done in the previous sections, the case of $Nc = 1$ will be used as an example. The general case is presented in the appendix.

To analyze mass balance, consider summation of all ELLAM equations. Summation of equations associated with test functions w_0^{n+1} through w_{E+1}^{n+1} results in the following expression.

$$\int_{x_0}^{x_E} u(x, t^{n+1})\,dx - \left[\int_{x_0}^{x_{E+1}^*} u(x, t^n)\,dx + \int_{x_{E+1}^*}^{x_E} u(x, t^n) w_{E+1}^{n+1}(x, t^n)\,dx\right] - \int_{t^n}^{t^{n+1}}\left[Vu(0, t) - D\frac{\partial u}{\partial x}(0, t)\right]dt + \int_{t_{E+1}^*}^{t^{n+1}}\left[Vu(l, t) - D\frac{\partial u}{\partial x}(l, t)\right]dt + \int_{t^n}^{t_{E+1}^*}\left[Vu(l, t) - D\frac{\partial u}{\partial x}(l, t)\right] w_{E+1}^{n+1}(x, t)\,dt - D\left(\frac{1}{\Delta x}\right)\int_{t^n}^{t_{E+1}^*} u(l, t)\,dt + D\left(\frac{1}{\Delta x}\right)\int_{t^n}^{t_{E+1}^*} u(x_c^{E+1}(t), t)\,dt = \int_{t^n}^{t^{n+1}}\int_{x_0}^{x_E} f(x, t)\,dx\,dt - \int_{\Omega_2^{E+1}} f(x, t)[1 - w_{E+1}^{n+1}(x, t)]\,dx\,dt. \quad (18)$$

In equation (18), use was made of the fact that within any space-time element $\Omega_1^k = \Omega_2^{k-1}$ and $w_k^{n+1} + w_{k-1}^{n+1} = 1$. In addition, $\Sigma_{i=0}^E w_i^{n+1}(x, t^{n+1}) = 1$ $(0 \le x \le l)$ and $\Sigma_{i=0}^E w_i^{n+1}(0, t) = 1$ $(t^n \le t \le t^{n+1})$. Examination of equation (18) indicates that a global balance is almost achieved, with boundary and interior regions associated with space-time element Ω_2^{E+1} being responsible for the lack of global balance. This can be explained as follows. Within any space-time element that is bounded by nodes x_k and x_{k+1} at time t^{n+1}, two test functions will be nonzero, namely w_k^{n+1} and w_{k+1}^{n+1}. Because these functions sum to one within the element, and because of the symmetries in the boundary integral terms, the sum of the two ELLAM equations associated with these two test functions preserves a global balance. Element Ω_2^{E+1} suffers from the lack of an ELLAM equation associated with test function $w_{E+2}^{n+1}(x, t)$. In fact, w_{E+2}^{n+1} is the only remaining test function that has a nonzero region in $[0, l] \times [t^n, t^{n+1}]$ for which an ELLAM equation has not been written. The ELLAM equation associated with w_{E+2}^{n+1} is not needed to solve for the nodal unknowns of interest, because the known values from the previous time level at node E in effect supersede this equation. However, this final equation can be used to enforce global mass conservation.

The test function $w_{E+2}^{n+1}(x, t)$ is illustrated in Fig. 6. The ELLAM equation associated with test function $w_{E+2}^{n+1}(x, t)$ is

$$\int_{t^n}^{t_{E+1}^*}\left[Vu(l, t) - D\frac{\partial u}{\partial x}(l, t)\right] w_{E+2}^{n+1}(l, t)\,dt - \int_{x_{E+1}^*}^{x_E} u(x, t^n) w_{E+2}^{n+1}(x, t^n)\,dx + D\left(\frac{1}{\Delta x}\right)\left[\int_{t^n}^{t_{E+1}^*} u(l, t)\,dt - \int_{t^n}^{t_{E+1}^*} u(x_l^{E+2}(t), t)\,dt\right] = \int_{\Omega_1^{E+2}} f(x, t) w_{E+2}^{n+1}(x, t)\,dx\,dt. \quad (19)$$

Summation of equations (18) and (18) yields

$$\int_{x_0}^{x_E} u(x, t^{n+1})\,dx - \int_{x_0}^{x_E} u(x, t^n)\,dx - \int_{t^n}^{t^{n+1}}\left[Vu(0, t) - D\frac{\partial u}{\partial x}(0, t)\right]dt + \int_{t^n}^{t^{n+1}}\left[Vu(l, t) - D\frac{\partial u}{\partial x}(l, t)\right]dt = \int_{t^n}^{t^{n+1}}\int_{x}^{x_E} f(x, t)\,dx\,dt, \quad (20)$$

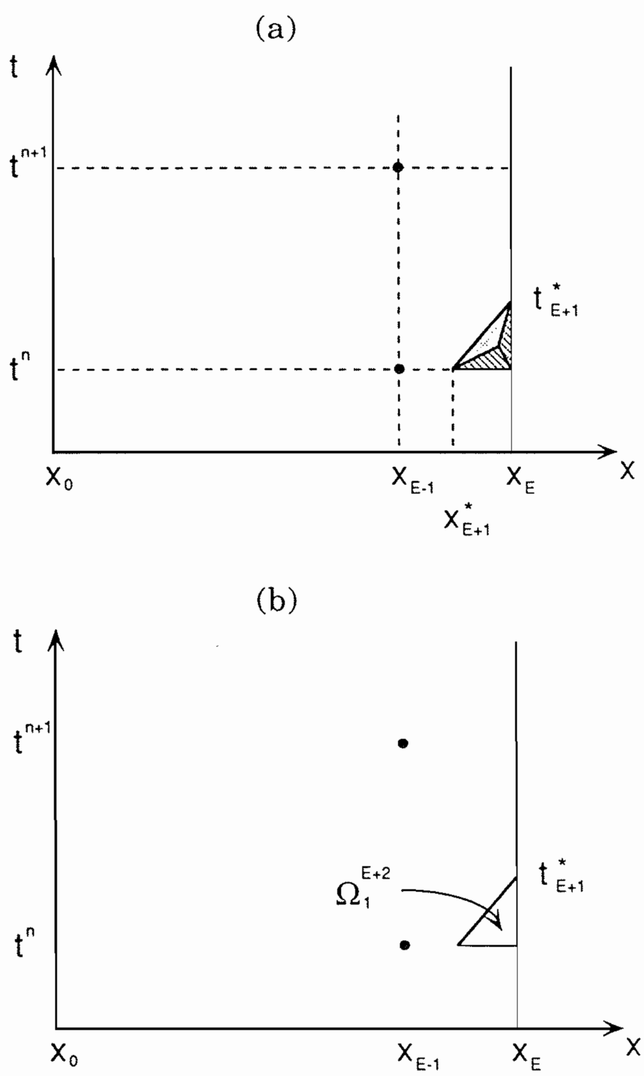

Fig. 6. (a) Test function $w^{n+1}_{E+2}(x, t)$, and (b) associated geometric definitions

which represents a statement of global mass conservation. Therefore, the set of all ELLAM equations, including that associated with $w^{n+1}_{E+2}(x, t)$, possesses the conservative property. However, use of all ELLAM equations over-specifies the system by one equation. Yet without equation (19), the ELLAM system does not, in general, possess the conservative property. Therefore, add equation (19) to equation (17), noting that $x_l^{E+2}(t) = x_c^{E+1}(t)$, $\Omega_1^{E+2} = \Omega_2^{E+1}$, and $w^{n+1}_{E+1}(x, t) + w^{n+1}_{E+2}(x, t) = 1$ on Ω_2^{E+1} (see Figs 5 and 6). This yields

$$\left[\int_{t^*_{E+1}}^{t^{n+1}}\left[Vu(l, t) - D\frac{\partial u}{\partial x}(l, t)\right]w^{n+1}_{E+1}(l, t)\,\mathrm{d}t\right.$$

$$\left.\int_{t^n}^{t^*_{E+1}}\left[Vu(l, t) - D\frac{\partial u}{\partial x}(l, t)\right]\mathrm{d}t\right]$$

$$-\left[\int_{x^*_E}^{x^*_{E+1}} u(x, t^n)w^{n+1}_{E+1}(x, t^n)\,\mathrm{d}x\right.$$

$$\left.+\int_{x^*_{E+1}}^{x_E} u(x, t^n)\,\mathrm{d}x\right]$$

$$+D\left(\frac{1}{\Delta x}\right)\int_{t^*_{E+1}}^{t^{n+1}} u(l, t)\,\mathrm{d}t$$

$$-D\left[\left(\frac{1}{\Delta x}\right)\int_{t^n}^{t^{n+1}} u(w_l^{E+1}(t), t)\,\mathrm{d}t\right.$$

$$\left.-\left(\frac{1}{\Delta x}\right)\int_{t^n}^{t^*_{E+1}} u(x_c^{E+1}(t), t)\,\mathrm{d}t\right]$$

$$= \int_{\Omega_1^{E+1}} f w^{n+1}_{E+1}\,\mathrm{d}x\,\mathrm{d}t + \int_{\Omega_2^{E+1}} f(x, t)\,\mathrm{d}x\,\mathrm{d}t. \qquad (21)$$

If equation (21) is used in place of equation (17), then the proper number of ELLAM equations results and these equations possess the conservative property by summing to equation (20) instead of equation (19).

The modifications presented above guarantee mass conservation for the system of equations that includes U_{α_1} as an unknown. Recall that this was one of two options presented in Section 4, the other being simple interpolation between t^n and t^{n+1} along the outflow boundary. If this other option is chosen, global mass conservation can still be achieved. This is accomplished by using the information contained in the ELLAM equations associated with w^{n+1}_{E+1} and w^{n+1}_{E+2}. In this case, these two equations (equations (17) and (19)) should be summed and then added to the equation associated with w_E^{n+1} (equation (16)) to obtain

$$\int_{x_{E-1}}^{x_E} u(x, t^{n+1})w_E^{n+1}(x, t^{n+1})\,\mathrm{d}x$$

$$+\int_{t^n}^{t^{n+1}}\left[Vu(l, t) - D\frac{\partial u}{\partial x}(l, t)\right]\mathrm{d}t$$

$$-\left[\int_{x^*_{E-1}}^{x^*_E} u(x, t^n)w_E^{n+1}(x, t^n)\,\mathrm{d}x\right.$$

$$\left.+\int_{x^*_E}^{x_E} u(x, t^n)\,\mathrm{d}x\right]$$

$$-D\left[\left(\frac{1}{\Delta x}\right)\int_{t^n}^{t^{n+1}} u(x_l^E(t), t)\,\mathrm{d}t\right.$$

$$\left.-\left(\frac{1}{\Delta x}\right)\int_{t^n}^{t^{n+1}} u(x_c^E(t), t)\,\mathrm{d}t\right]$$

$$= \int_{\Omega_1^E} f w_E^{n+1}\,\mathrm{d}x\,\mathrm{d}t + \int_{\Omega_1^{E+1}\cup\Omega_1^{E+2}} f\,\mathrm{d}x\,\mathrm{d}t. \qquad (22)$$

Just as equation (19) modified equation (17) to provide a conservative scheme when U_{α_1} was included, now the sum of equations (17) and (19) injects information into equation (16) so that global mass conservation is guaranteed.

In general, ELLAM equations should be written for all test functions that have nonzero values within $[x_0, x_E] \times [t^n, t^{n+1}]$. For the case of $Nc = 1$, this means w_0^{n+1}

through w_{E+2}^{n+1}. If a first-type boundary condition is given at the outflow boundary, then the first E equations may be solved independently. If detailed information about $(\partial u/\partial x)$ at the outflow boundary is desired, then the additional equations should be written and solved for nodal values of $(\partial U_E^{n+1}/\partial x)$ and $(\partial U_{\alpha_1}/\partial x)$, subject to the global conservation constraint imposed by the equation associated with w_{E+2}^{n+1}. If only a measure of the total flux crossing the boundary is of interest, the additional equations may be summed to give a relationship between total outflux and known information. For the case of $Nc = 1$, rearrangement of equation (22) yields

$$\begin{aligned}\int_{t^n}^{t^{n+1}} \left[Vu(l, t) - D\frac{\partial u}{\partial x}(l, t) \right] \mathrm{d}t &= \int_{\Omega_1^E} f w_E^{n+1} \,\mathrm{d}x\,\mathrm{d}t \\ &+ \int_{\Omega_1^{E+1} \cup \Omega_1^{E+2}} f(x, t)\,\mathrm{d}x\,\mathrm{d}t \\ &+ D\left[\left(\frac{1}{\Delta x}\right) \int_{t^n}^{t^{n+1}} u(x_l^E(t), t)\,\mathrm{d}t \right. \\ &\left. - \left(\frac{1}{\Delta x}\right) \int_{t^n}^{t^{n+1}} u(x_c^E(t), t)\,\mathrm{d}t \right] \\ &+ \int_{x_{E-1}^*}^{x_E^*} u(x, t^n) w_E^{n+1}(x, t^n)\,\mathrm{d}x \\ &+ \int_{x_E^*}^{x_E} u(x, t^n)\,\mathrm{d}x \\ &- \int_{x_{E-1}}^{x_E} u(x, t^{n+1}) w_E^{n+1}(x, t^{n+1})\,\mathrm{d}x. \qquad (23)\end{aligned}$$

All information on the right side of equation (23) is known from the previous solution of the first E ELLAM equations, so that the total flux may be calculated.

For a second- or third-type boundary condition at the outflow boundary, the equation associated with w_E^{n+1} must be written. Evaluation of the boundary flux terms may then proceed by introduction of the additional unknown U_{α_1}, as illustrated in Section 4, or by interpolation between time levels n and $n + 1$. If the latter case is chosen, then equation (16) would be replaced by equation (22). Otherwise, equation (19) is summed with equation (17) as demonstrated in equation (21). In all of these cases, global mass conservation is assured.

Notice that summation of equations produces a result that is equivalent to deriving the ELLAM equations using a redefined test function. This redefined test function is equal to the sum of the original test functions. For example, combination of equations (17) and (19) results in equation (21); equation (21) can also be obtained by application of ELLAM using the modified test function $w^* \equiv w_{E+1}^{n+1} + w_{E+2}^{n+1}$, which has the definition,

$$w^*(x, t) = \begin{cases} \dfrac{x - x_E}{\Delta x} + \dfrac{t^{n+1} - t}{\Delta x}, & (x, t) \in \Omega_1^{E+1}, \\ 1 \quad , & (x, t) \in \Omega_2^{E+1}, \\ 0, \quad , & \text{all other } (x, t). \end{cases}$$

Similarly, the combination of equations (16), (17), and (19) (which eliminates U_{α_1}) can be achieved using ELLAM with test function $w^{**} \equiv w_E^{n+1} + w_{E+1}^{n+1} + w_{E+2}^{n+1}$,

$$w^{**}(x, t) = \begin{cases} \dfrac{x - x_{E-1}}{\Delta x} + \dfrac{t^{n+1} - t}{\Delta x}, & (x, t) \in \Omega_1^E, \\ 1 \quad , & (x, t) \in \Omega_2^E \text{ or } (x, t) \in \Omega_2^{E+1}, \\ 0 \quad , & \text{all other } (x, t). \end{cases}$$

The redefined test functions still satisfy the homogeneous adjoint equation within each element.

While the ELLAM procedure provides a variety of choices for dealing with boundary conditions, the procedure can always incorporate all types of possible boundary conditions and guarantee that a conservative scheme will result. In general, when a first-type boundary condition is given at the inflow boundary, equations associated with w_0^{n+1} and w_i^{n+1} $(1 \le i < E)$ should be written. The first $Nc + 2$ of these equations will include boundary values of both u and $(\partial u/\partial x)$. When a one-point fully implicit approximation is used for these boundary integrals, the flux integral only appears in the first (w_0^{n+1}) equation, so that it is not necessary to solve for the unknown $(\partial u/\partial x)$ at t^{n+1}. The ELLAM equation associated with w_0^{n+1} is uncoupled from the others in this case, and only needs to be used to calculate the inflow boundary flux, if desired. As in the outflow case just described, this may be done by replacing w_1^{n+1} with the sum $w_0^{n+1} + w_1^{n+1}$, which is equal to one on Ω_1^1. When a second- or third-type boundary condition is specified at the inflow boundary, the equation associated with w_0^{n+1} must be used, independent of the boundary integration method chosen. The outflow boundary is similar to the inflow boundary in that no boundary equations are required when a first-type condition is specified. Boundary equations, associated with w_E^{n+1}, w_{E+1}^{n+1}, . . . , are required only to calculate the associated outflow boundary flux. For flux boundary conditions, at least one outflow boundary equation must be written, that being the equation based on the summed test functions. If more refined information is desired at the outflow boundary, individual equations may be written for w_E^{n+1}, w_{E+1}^{n+1}, . . . , with concomitant introduction of additional unknowns analogous to U_{α_1} above. These procedures yield Eulerian-Lagrangian schemes that demonstrably possess the conservative property.

A final consideration in boundary condition implementation is the matrix structure of the resulting set of algebraic equations. This depends on the choice of trial function, call it $\hat{u}$, that is used to approximate the unknown function u. So far, the trial function has not been specified, except in the MMOC example of equation (13). In view of the test functions, which have the chapeau form at $t = t^{n+1}$, it is natural to define $\hat{u}$ to be piecewise linear also. Interpolation between $t = t^n$ and $t = t^{n+1}$ can be taken to be linear along characteristic lines. For one-space-dimensional problems, this gives rise to the general matrix structure illustrated in Fig. 7. The matrix is symmetric, tridiagonal except for the additional column of potentially nonzero entries associated with inflow boundary information. This corresponds to the unknown at the inflow

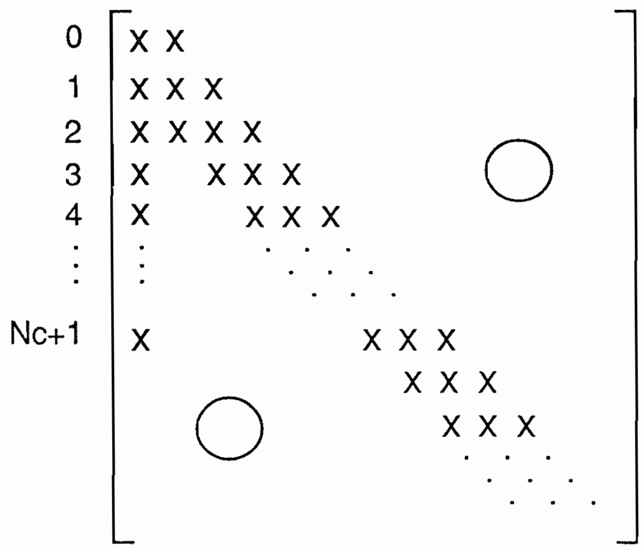

Fig. 7. General matrix structure for ELLAM. Nc is the truncated integer value of the Courant number

boundary: $(\partial U_0^{n+1}/\partial x)$ for Dirichlet problems and U_0^{n+1} for Neumann or Robin problems. This column (except for the entry in row one) may be eliminated in the Dirichlet problem via judicious one-point approximations to the integrals involving $(\partial u/\partial x)(0, t)$. Elimination of this column is more difficult in the other cases of second- or third-type boundary conditions because it appears that larger errors are committed in achieving this, although quantitative demonstration of this point remains to be done.

Notice that the matrix structure depends entirely on the chosen interpolation (integration) rule, which is dictated by choice of trial function. For example, a space-time interpolation that does not follow characteristic lines will in general lead to less sparseness in the matrix stucture, accompanied by loss of symmetry. This is an important consideration because the computational advantages in maintaining a symmetric tridiagonal matrix are significant, while the accuracy of the method depends heavily on the chosen interpolation. Further analysis is required to adequately resolve this issue.

6. THE CASE OF PURE ADVECTION

The ELLAM equations presented in Sections 3 through 5 naturally accommodate the degenerate case of $D = 0$. The approach incorporates all of the space-time domain of interest and uses known information from the previous time step (U_E^n) to close the system of discrete equations. The ELLAM equations remain exactly as written in Sections 3, 4, and 5, with any terms multiplied by D simply set to zero. All terms involving spatial gradients $(\partial u/\partial x)$ disappear because they are all multiplied by D (actually these terms never arise because the second-order diffusive term is absent in the governing equation). Unknowns are now $\{U_1^{n+1}, U_2^{n+1}, \ldots, U_E^{n+1}, U_{\alpha_1}\}$ (assuming $Nc = 1$). A first-type boundary condition is required at $x = 0$, since the governing equation is now formally first-order. Therefore U_0^{n+1} will be known. Notice that the test functions continue to satisfy the homogeneous adjoint equation within each space-time element. This is why the ELLAM equations can be used directly as written above. The ELLAM equations therefore inherently accommodate a formal change of governing from a second-order parabolic equation in which boundary conditions are specified at both inflow and outflow boundaries to a first-order hyperbolic equation in which boundary conditions are given only at inflow boundaries. No change is required in the ELLAM algorithm.

7. EXAMPLE CALCULATIONS

This section reports on computations with ELLAM for a simple test problem. As noted in Section 3, a backward Euler approximation of the temporal integrals in interior elements yields the MMOC procedure, given by equation (13). The benefit of ELLAM in this context is that it shows how to treat boundary conditions (Section 4) and conserve mass (Section 5). Numerical results applying MMOC to equation (3) have appeared previously[22], but that work did not address boundary conditions, since the computational boundaries were far from the advecting front. Hence, mass conservation, which did hold in the earlier work, was not studied in a situation where boundaries were important.

With this background, the natural experiments to perform here are ones that include significant boundary behaviour. We consider an advecting Gaussian hill that may cross an inflow or outflow boundary. Specifically, we solve equation (3) with $f = 0$ and initial condition

$$u_I(x) = \exp(-\pi x^2) \tag{24}$$

chosen so that the initial peak value of u and total mass are both equal to 1. As a pure initial-value problem, this leads to the analytical solution

$$u_a(x, t) = \frac{1}{\sqrt{1 + 4\pi Dt}} \exp\left(\frac{-\pi(x - Vt)^2}{1 + 4\pi Dt}\right). \tag{25}$$

We obtain an initial-boundary-value problem with the same solution by cutting off the spatial domain and imposing Dirichlet or flux boundary conditions from equation (25), viz.,

$$u(a, t) = u_a(a, t)$$

or

$$\left(Vu - D\frac{\partial u}{\partial x}\right)(a, t) = \left(Vu_a - D\frac{\partial u_a}{\partial x}\right)(a, t), \tag{26}$$

$$u(b, t) = u_b(b, t),$$

or

$$\left(Vu - D\frac{\partial u}{\partial x}\right)(b, t) = \left(Vu_a - D\frac{\partial u_a}{\partial x}\right)(b, t), \tag{27}$$

where $\Omega_x = [a, b]$ is the truncated spatial domain.

In the runs to be reported here, we used $V = 10$, $D = 0.1$, and final time $t_f = 0.5$. Thus, the peak traveled from $x = 0$ to $x = 5$, over which distance the Peclet number was 500. Some runs with $D = 0.001$, or Peclet number 50,000, were also made. The exact solutions in these cases are shown in Fig. 8. We considered the

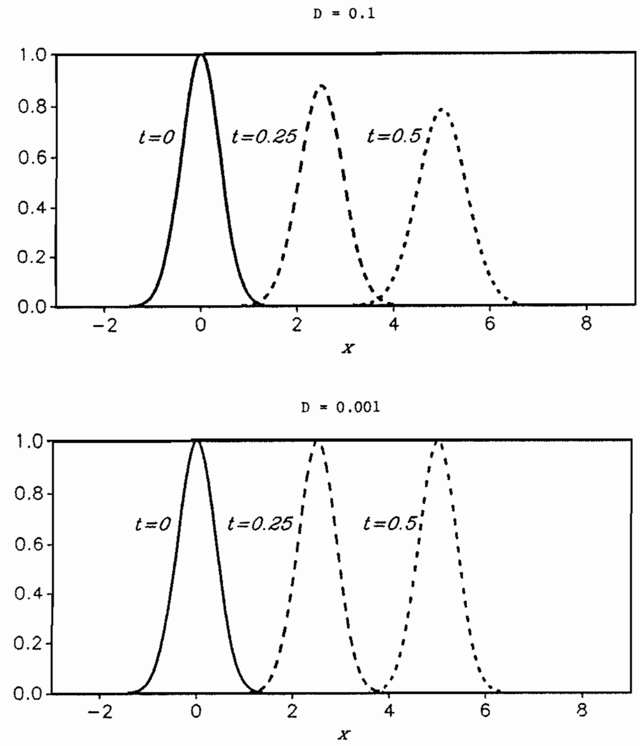

Fig. 8. Exact solution for example problem (equation (25)) with (a) $D = 0.1$, and (b) $D = 0.001$

domains $[2\frac{1}{3}, 9]$, $[-3, 2\frac{1}{3}]$, and $[-3, 9]$, with which, respectively, the pulse crosses an inflow boundary, an outflow boundary, or neither; denote the domains by I, O, and N. For each domain, all relevant combinations of boundary conditions were tried. The maximum slope of the initial pulse is $\sqrt{2\pi/e} \approx 1.52$, and at $t = t_f$ it is $\sqrt{(2\pi/e)/(1 + 4\pi D t_f)} \approx 0.933$ $(D = 0.1)$ or 1.51 $(D = 0.001)$ with peak value $1/\sqrt{1 + 4\pi D t} \approx 0.784$ $(D = 0.1)$ or 0.997 $(D = 0.001)$.

Previous numerical studies of MMOC with linear trial functions have demonstrated that it produces accurate, nonoscillatory results as long as at least three intervals discretize a front. In the context of a Gauss hill of peak value 1, we take this to mean that Δx should be no larger than $1/3S$, were S is the maximum slope; in our case this is $\sqrt{e/18\pi} \approx 0.219$. Our runs showed that we could do slightly better than this, and $\Delta x = 4/15 \approx 0.267$ was used as a base case. This corresponds to a grid Peclet number $Pe = V\Delta x/D = 26\frac{2}{3}$. As a check on convergence rates, we also ran with the 5-fold refinement $\Delta x = 4/75 \approx 0.0533$ $[Pe = 5\frac{1}{3}]$. For $\Delta x = 4/15$, we used $\Delta t = 0.25$ and 0.05 (Cu $= 9\frac{3}{8}, 1\frac{7}{8}$); for $\Delta x = 4/75$, $\Delta t = 0.25$, 0.05, 0.01, and 0.002 (Cu $= 46\frac{7}{8}, 9\frac{3}{8}, 1\frac{1}{7}, \frac{3}{8}$) were run.

In order to assess the effectiveness of ELLAM in the absence of quadrature errors, we computed integrals involving initial and boundary conditions with high-order Lobatto rules. For example, in equation (14), the second integral involves initial conditions when $n = 0$, and the third and seventh integrals combine into a flux boundary condition (for a Dirichlet condition, the third integral uses the boundary data, while the seventh becomes a spatial integral at time level $n + 1$ under a backward Euler scheme detailed in Ref. 43). Similarly, in equation (17), the first, second, and fifth integrals are of these types, and the second integral in equation (9) uses $u_I(x)$ when $n = 0$. For $n > 0$, as noted in Section 3, the integrals at $t = t^n$ can be evaluated exactly, and this was done here. Integrals such as the first in equation (9) were computed exactly, and temporal integrals were replaced by backward Euler approximations in order to obtain the MMOC procedure. With these specifications, all calculations conserved mass to the level of machine roundoff.

In the computations, we found it advantageous to consolidate the last two outflow-boundary elements described in Section 4 into a single element. That is, instead of Nc trapezoids and one small triangle along the outflow boundary, we have $Nc - 1$ trapezoids and one larger triangle. This corresponds to use of the function w^{**} in Section 5, and avoids the possibility of anomalous answers on the small triangle. For a Dirichlet outflow condition, as noted in Section 5, ELLAM solves for the outgoing flux as a function of time; we considered piecewise-linear and piecewise-constant representations of this function. For full details of the implementation, see Ref. 43.

Results for the test runs are summarized in Table 1. All runs used $D = 0.1$ except for those designed by 'd', which took $D = 0.001$. For the domains N and I, L^2 errors and peak values are given at the final time $t_f = 0.5$. For O, these are listed at $t = 0.25$, at which time the peak is leaving the domain. This time usually provided the least favorable (i.e., largest) ratio of the L^2 error of the numerical solution to that of the L^2 projection; this ratio is necessarily at least 1. In runs 25 through 30, the peak has left and the Dirichlet outflow condition forces the numerical maximum to agree with the exact one, rendering peak-value data meaningless.

Runs 1 through 6 do not involve significant boundary behaviour, so that the implemented ELLAM reduces to MMOC and we find results analogous to those reported by Ewing and Russell[22]. Comparing runs 5 and 6, we see that temporal error is relatively unimportant, so that we can conclude $0(\Delta x^2)$ convergence by relating run 1 to 5 or 2 to 6. Similarly, spatial error is unimportant in runs 3 and 4 and we find a rate of $0(\Delta t)$. Runs 1 and 2, with a spatial mesh of the size that one would want in practice, show that large Courant numbers are appropriate with this scheme. The peak in excess of 1 in run $2d$ is not an instability; as the L^2 projection shows, it is a necessary result of accurate approximation of a peak by continuous piecewise-linear polynomials on a course grid. By examining the difference between the numerical peak value and the L^2-projection peak for fixed Δx and variable Δt, we see that time truncation is antidiffusive; with variable Δx and fixed Δt, spatial error is found to be diffusive.

Runs 7 through 18, with domain I, demonstrate that we can move the peak through the inflow boundary about as well as possible. Comparison of runs 7 through 12, as a group, to 13 through 18 shows that the type of boundary condition makes virtually no difference. The L^2 error tends to be slightly larger with a Dirichlet condition, especially in the lower-diffusion run 8d. This is easily explained by noting that the essential condition is imposed exactly at the boundary node, while better L^2 accuracy during the passage of the peak could be obtained if the boundary value were free as in the flux-condition case. For related reasons, runs 8 and 8d show miniscule oscillations (of size about 0.0001 and 0.001, respectively) ahead of the peak as it enters; diffusion subsequently eliminates

Table 1 Numerical results on the domain $[x_0, x_E]$

Run	Domain	Boundary		Δx	Δt	L^2 error*		Peak Value*		
		In	Out			L^2 proj	num sol	L^2 proj	num sol	exact
1	N	D	F	0.267	0.250	7.15E−3	1.06E−2	0.802	0.813	0.784
2	N	D	F	0.267	0.050	7.15E−3	8.92E−3	0.802	0.795	0.784
2d	N	D	F	0.267	0.050	1.37E−2	1.47E−2	1.035	1.029	0.997
3	N	D	F	0.053	0.250	2.65E−4	1.49E−2	0.784	0.803	0.784
4	N	D	F	0.053	0.050	2.65E−4	3.11E−3	0.784	0.788	0.784
5	N	D	F	0.053	0.010	2.65E−4	4.51E−4	0.784	0.785	0.784
6	N	D	F	0.053	0.002	2.65E−4	4.20E−4	0.784	0.784	0.784
7	I	D	F	0.267	0.250	7.15E−3	7.92E−3	0.802	0.806	0.784
8	I	D	F	0.267	0.050	7.15E−3	8.22E−3	0.802	0.797	0.784
8d	I	D	F	0.267	0.050	1.37E−2	1.78E−2	1.035	1.032	0.997
9	I	D	F	0.053	0.250	2.65E−4	6.95E−3	0.784	0.793	0.784
10	I	D	F	0.053	0.050	2.65E−4	1.63E−3	0.784	0.786	0.784
11	I	D	F	0.053	0.010	2.65E−4	3.23E−4	0.784	0.785	0.784
12	I	D	F	0.053	0.002	2.65E−4	3.04E−4	0.784	0.784	0.784
13	I	F	F	0.267	0.250	7.15E−3	7.82E−3	0.802	0.807	0.784
14	I	F	F	0.267	0.050	7.15E−3	7.71E−3	0.802	0.798	0.784
14d	I	F	F	0.267	0.050	1.37E−2	1.40E−2	1.035	1.031	0.997
15	I	F	F	0.053	0.250	2.65E−4	6.90E−3	0.784	0.793	0.784
16	I	F	F	0.053	0.050	2.65E−4	1.63E−3	0.784	0.786	0.784
17	I	F	F	0.053	0.010	2.65E−4	3.29E−4	0.784	0.785	0.784
18	I	F	F	0.053	0.002	2.65E−4	3.18E−4	0.784	0.784	0.784
19	O	D	F	0.267	0.250	4.97E−3	7.16E−3	0.833	0.849	0.816
20	O	D	F	0.267	0.050	4.97E−3	6.11E−3	0.833	0.823	0.816
20d	O	D	F	0.267	0.050	6.79E−3	6.95E−3	0.936	0.932	0.915
21	O	D	F	0.053	0.250	1.77E−4	7.88E−3	0.817	0.841	0.816
22	O	D	F	0.053	0.050	1.77E−4	2.17E−3	0.817	0.826	0.816
23	O	D	F	0.053	0.010	1.77E−4	3.70E−4	0.817	0.819	0.816
24	O	D	F	0.053	0.002	1.77E−4	4.39E−4	0.817	0.814	0.816
25	O	D	D	0.267	0.250	4.97E−3	9.13E−3			
26	O	D	D	0.267	0.050	4.97E−3	7.15E−3			
26d	O	D	D	0.267	0.050	6.79E−3	8.98E−3			
27	O	D	D	0.053	0.250	1.77E−4	5.89E−3			
28	O	D	D	0.053	0.050	1.77E−4	1.19E−3			
29	O	D	D	0.053	0.010	1.77E−4	2.48E−4			
30	O	D	D	0.053	0.002	1.77E−§	2.43E−4			

*At $t = 0.5$ for domain N or I, $t = 0.25$ for domain O

them in run 8, while they grow to size 0.002 in run 8d. These oscillations are attributable to the Dirichlet condition, as just noted, and the coarseness of the grid; they disappear in run 10 and in an analogous refinement of run 8d, and they are absent in runs 14 and 14d. Comparing 7−12 and 13−18 to runs 1 through 6, it is interesting that the errors are generally smaller and the peak values closer to those of the L^2 projection. This apparently happens because the incoming peak is defined analytically by boundary data and has less time to accumulate errors than in the N runs. The results support the contention that ELLAM formulates the 'correct' approach to inflow boundaries in MMOC, and by extension, in ELM.

Runs 19 through 30, with domain 0, also compare well to runs 1 through 6 in the domain $[x_0, x_E]$. No appreciable oscillations appeared in any of these runs. The only case in which the L^2 error is noticeably worse than in the N runs is run 26d, where the Dirichlet outflow condition has an effect analogous to that of the inflow condition in run 8d.

We conclude this section with a discussion of the discretized outflow boundary, where the results raise some questions. If we have a flux condition, we solve for U_E^{n+1}, $U(x_E, t_{E+1}^*)$, . . . , $U[x_E, t_{E+Nc-1}^*]$, regarding U as piecewise-linear. With Dirichlet data, we solve instead for $\partial U/\partial x(x_E, t^{n+1})$, $\partial U/\partial x(x_E, t_{E+1}^*)$, . . . , $\partial U/\partial x[x_E, t_{E+Nc-1}^*]$, where $\partial U/\partial x$ is taken to be piecewise-linear, in which case the known $\partial U/\partial x(x_E, t^n)$ completes the solution, or piecewise-constant, where $\partial U/\partial x(x_E, t) = \partial U/\partial x(x_E, t_j^*)$ for $t_{j+1}^* < t \leq t_j^*$. When $\mathrm{Cu} \geq 2$, we can examine the behaviour of the solution at x_E as a function of t within a time step, while for $\mathrm{Cu} < 2$ we can study the solution over multiple steps.

Runs 19 through 24, with a flux condition, were mostly well-behaved. At time 0.25, run 19 showed an oscillation of order 0.01 in the outflow values closest to t^n, an effect that disappeared with the smaller time step of run 20 or 20d. Run 21 experienced larger wiggles of order 0.1 at time 0.25, which likewise were absent in runs 22, 23, and 24. The L^2 errors indicate that the time step of run 21 is simply too large to lead to accurate results. In the runs with more than two time steps (20, 22, 23, and 24), the outlet value was a smooth function of t across multiple steps. We view these results positively, though better understanding of the causes of the oscillations in cases like run 19 is desirable.

The Dirichlet condition of runs 25 through 30 gives rise to greater difficulties. With piecewise-linear outlet flux, runs 25, 27, and 28 oscillate badly within a time step, and run 26 does the same across multiple steps. The finely discretized runs 29 and 30 yield good results. The situation with piecewise-constant flux is considerably better, with all $D = 0.1$ runs producing reasonable answers. The runs with two time steps (25 and 27) obtain a maximum U_x that is too large, possibly because of the antidiffusive nature of time truncation. Ahead of the peak, run 26 has a small oscillation in t over multiple time steps. Otherwise, the results for $D = 0.1$ are qualitatively and quantitatively accurate. In run 26d, with $D = 0.001$, the computed values of U_x had more pronounced oscillations than those in run 26, and the values were much too large.

The effects just described appear to arise from forms of ill-conditioning in the discrete equations. If the outlet flux is peicewise-linear, a vector of alternating $+1$'s and -1's almost solves the associated homogeneous equations; only in the first and last equations, which receive information from the values at t^{n+1} and t^n, respectively, does it fail. This vector corresponds to a net flux of zero from each boundary element, so it presents no problem in the piecewise-constant equations. The trouble with $D = 0.001$ is that the matrix entries for Dirichlet outflow elements contain a factor of D, while the right-hand side involves the difference between the Dirichlet data and the approaching numerical solution, raising the possibility of a numerical boundary layer in time at the outlet. Artifices such as temporal 'upwinding' at the outflow boundary and imposition of Dirichlet data via penalties may be necessary to resolve these questions. The discretized outflow boundary will be addressed more thoroughly in future work.

8. DISCUSSION AND EXTENSIONS

The ELLAM approximations presented above provide a systematic framework for development of characteristic methods (CM's) for numerical approximation of advective-diffusive transport equations. The LAM philosophy leads naturally to the definition of special space-time test functions that produce the generalized CM approximations. The resulting set of approximating equations subsumes many of the CM approximations proposed in the literature. It therefore unifies these sometimes diverse methods. In addition, the development inherently provides a systematic procedure for proper incorporation of all types of boundary conditions in a mass-conservative scheme.

Most previous work is based on the operator splitting concept inherent in ELM or MMOC. This is distinct from ELAM, which is based on a space-time finite element concept. We are aware of several other uses of space-time finite elements for advection-diffusion transport, including the finite element method incorporating characteristics (FEMIC) of Varoglu and Finn[47], the streamline diffusion (SD) method of Brooks and Hughes[7], and a characteristic finite element method reported in Benque and Ronat[4]. FEMIC uses test functions that are analogous to ELLAM in that the space-time elements align with the characteristics. However, FEMIC uses forward tracking, which gives rise to the usual difficulties of distorted grids, while ELLAM uses backward tracking. In addition, the treatment of boundary conditions in FEMIC employs one triangular space-time element at the boundary, which effectively limits the Courant number to be of order 1. ELLAM has no such restrictions. Overall, the ELLAM approach to boundary condition implementation is much more general than FEMIC. The SD scheme is based on the addition of an optimal amount of artificial diffusion. In addition, the space-time elements are not necessarily aligned with the characteristics[36]. Benque and Ronat[4] use the idea of a locally vanishing adjoint to define test functions, although they only consider the advective component of the equation. In addition, a domain extension concept is used to treat inflow boundaries. It appears that this boundary treatment neglects the spatial dependence of the effective time step over which diffusion acts, as discussed above in the context of general Eulerian Lagrangian methods. This also fails to give rise to a diffusive flux term at the physical boundary, thereby making enforcement of mass balance difficult in the general advection-diffusion case. Later applications of the method of Benque and Ronat (for example by Hervouet[31]) continue to focus only on advective transport and therefore do not treat the general problem that we have considered herein.

Treatment of boundary conditions in other characteristic methods can also be compared to ELLAM, insofar as the other treatments can be interpreted. It appears that most methods are restricted to first-type inflow conditions, using the boundary value at the characteristic intersection of the boundary. No account it taken of the fact that the effective time step is less than Δt ($t^{n+1} - t_1^*$ in Section 4), except in the work of Douglas *et al.*[20], in which the x-dependence at Δt is included. Neuman[38] and Neuman and Sorek[39] present explicit procedures for incorporating boundary conditions into their split equations, but the resulting equations do not appear to possess the conservative property. The ELLAM formulation, which is based on systematic space-time integration, appears to be the approach that is closest to the physical origins of the differential equation; individual terms can be interpreted as interior changes in mass, boundary fluxes, and external sources/sinks. All boundary conditions are naturally accommodated, in particular flux conditions. This systematic treatment of boundary conditions, which gives rise to a conservative numerical approximation, appears to be the first complete treatment of boundary conditions for Eulerian-Lagrangian methods.

There are many extensions that may be contemplated for the LAM algorithms. For example, application of the procedures to transport problems in multiple spatial dimensions may be accomplished by using the same order-of-derivative splitting concepts introduced above for the adjoint operator solutions. This leads to solutions (test functions) that follow the multi-dimensional characteristic curves in space-time, while simultaneously satisfying the diffusive part of the operator. The latter (diffusion) solution might naturally use the tensor product functions employed by Celia *et al.*[12]. The resulting space-time ELLAM equations would be analogous to the one-dimensional equations, including implementation of boundary conditions.

Development of higher-order approximations might proceed along several lines. First, higher-order estimates can be used to approximate the line integrals that appear in the LAM equations. This may be achieved, for example, by using high order interpolates for the function $u(x, t^n)$, many forms of which have been investigated by Baptista[3]. Similarly, higher-order interpolates may be used for $u(x, t^{n+1})$, as well as the values of u along the characteristics. A second approach might be to use test functions that are higher-order polynomials (higher than linear). While this is possible, it is somewhat contrary to the spirit of the LAM development in that the test functions may no longer satisfy the homogeneous adjoint operator. Examination of equation (8) reveals that the interior integrations involving $\mathcal{L}^*w$ would then need to be evaluated, since $\mathcal{L}^*w \neq 0$. This is computationally straightforward, so that implementation of this option is computationally viable. The relative merits of these and other options remain to be fully explored.

ELLAM developments for reactive transport problems may also be derived. If equation (1) is modified to include a first order reaction term, viz.

$$\frac{\partial u}{\partial t} + V\frac{\partial u}{\partial x} - D\frac{\partial^2 u}{\partial x^2} + ku = f(x, t),$$

then treatment of the reaction term in the adjoint solution becomes necessary. In the context of ELLAM, the term Ku may be included with the first order terms or it may be included with the diffusive term. If included with the diffusive term, then the spatial part of the solution will be modified to satisfy the equation

$$D\frac{d^2w}{dx^2} - Kw = 0$$

so that $w = [\pm(K/D)^{1/2}x]$. The advective portion remains unchanged. Conversely, inclusion of the reaction term with the first order terms requires the test function to satisfy

$$\frac{\partial w}{\partial t} + V\frac{\partial w}{\partial x} - Kw = 0,$$

which leads to a solution that changes exponentially along the characteristics. We expect that the latter approach will provide the better approximation, although this remains to be explored.

Finally, we recognize that ELLAM will not develop into a general tool unless the case of variable coefficients is adequately addressed. We are in the initial stages of investigation, and offer the following observations. One of the significant problems in solving variable coefficient equations is accurate backtracking along characteristics. This problem is common to all ELM and MMOC methods, so that ELLAM can build upon the experiences reported in the literature (e.g., Refs 3 and 45). However, we feel that LAM procedures can offer additional advantages in that ideas from ELLAM can be combined with earlier Eulerian developments based on LAM, namely the optimal test function (OTF) concepts of Celia *et al.*[12,13]. For example, the advection term may be broken into two parts, one of which is an 'average' velocity over $[t^n, t^{n+1}]$, the other being the deviation from this average. The average advection term could be treated using ELLAM, with the remaining velocity component incorporated into the spatial (diffusive) part of the test function, thereby imparting a directional spatial bias to the test functions. In this way, simpler backtracking techniques can be employed, based on the average value of velocity, with the spatial asymmetry in the test function acting as a corrector for the less accurate tracking. An important advantage of this approach is that the residual advection would remain as part of the Eulerian equations, so that inaccuracies in tracking would not result in failure to conserve mass. Similar techniques, involving spatial asymmetries in the test function, can also be used to deal with nonconstant diffusion coefficients. These concepts have already been used with some success by Espedal and Ewing[21] and by Dahle *et al.*[15,16]. Analogous arguments apply for ELLAM approximations to nonlinear equations. The choice of linearization method will be important, as it is for all numerical approximations to nonlinear equations. However, once a linearization has been applied, the resulting equation is analogous to a nonconstant-coefficient problem. The discussions presented above are therefore directly pertinent for ELLAM approximations to nonlinear equations. In addition, recent experience in aplication of MMOC to nonlinear equations (see, for example, Refs 16 and 21) provides a basis for ELLAM derivations. We are currently investigating ELLAM approximations for several nonlinear problems.

9. CONCLUSION

This paper has presented a space-time localized adjoint method (LAM) approximation for the advection-diffusion transport equation. The formulation is based on a space-time discretization in which specialized test functions are defined. These functions locally satisfy the homogeneous adjoint equation within each element. The formulation leads to a general approximation that subsumes many specific methods based on combined Lagrangian and Eulerian approaches, so-called characteristic methods (CM's). We refer to this method as an Eulerian-Lagrangian localized adjoint method (ELLAM). The ELLAM approach not only provides a unification of CM methods, but also provides a systematic framework for incorporation of boundary conditions in CM approximations. Any type of boundary conditions can be accommodated, and the resulting ELLAM equations are demonstrably mass conservative. This appears to be the first complete treatment of boundary conditions in Eulerian-Lagrangian Methods that leads to a conservative scheme for the general transport equation.

Example calculations were presented to demonstrate that the ELLAM procedure can in fact handle all types of boundary conditions. Inflow boundary conditions were easily handled, but a few of the test cases indicate that additional analysis is required to fully understand the treatment of outflow boundaries. The ELLAM approach appears to have enormous potential in that it subsumes ELM and MMOC formulations, and can therefore draw on the vast experiences reported using these metods to formulate approximations. However, it opens many new possibilities by providing a systematic treatment of the entire space-time equation. While much remains to be done, it appears that extensions such as incorporation of reaction terms and treatment of nonconstant coefficients fit naturally into the formulation. In addition, combination of the ELLAM concepts with the optimal test function (OTF) method may offer further advantages in solving complex transport equations.

ACKNOWLEDGEMENTS

This work was supported in part by the National Science Foundation under Grants 8657419-CES and DMS-8821330, by the Institute for Scientific Computing through NSF Grant No. RII-8610680, and by the Environmental Protection Agency under Assistance Agreement CR 814945 to Princeton University. The authors gratefully acknowledge the assistance of Simon Zisman in preparing the manuscript.

Although the research described in this article has been funded in part by the U.S. Environmental Protection Agency, it has not been subjected to Agency review and therefore does not necessarily reflect the views of the Agency and no official endorsement should be inferred.

REFERENCES

1 Allen, D. and Southwell, R. Relaxation methods applied to determining the motion in two dimensions of a fluid past a fixed cylinder, *Quart. J. Mech. Appl. Math.*, 1955, **8**, 129–145

2 Barrett, J. W. and Morton, K. W. Approximate symmetrization and Petrov-Galerkin methods for diffusion-convection problems, *Comp. Meth. Appl. Mech. Engng.*, 1984, **45**, 97–122

3 Baptista, A. M. *Solution of Advection-Dominated Transport by Eulerian-Lagrangian Methods using the Backward Methods of Characteristics*, Ph.D. Thesis, Dept. Of Civil Engineering, M.I.T., 1987

4 Benque, J. P. and Ronat, J. Quelques difficultes des modeles numeriques en hydraulique, *Computing Methods in Applied Sciences and Engineering*, V, Glowinski and Lions (eds.) North-Holland, 471–494, 1982

5 Bouloutas, E. T. and Celia, M. A. An analysis of a class of Petrov-Galerkin and Optimal Test Functions methods, *Proc. Seventh Int. Conf. Computational Methods in Water Resources* Celia *et al.* (eds), 15–20, 1988

6 Bouloutas, E. T. and Celia, M. A. An improved cubic Petrov-Galerkin method for advection-dominated flows in rectangularly decomposable domains, to appear in *Comp. Meth. Appl. Mech. Engng.*, 1990

7 Brooks, A. and Hughes, T. J. R. Streamline upwind Petrov-Galerkin formulations for convection dominated flows with particular emphasis on the incompressible Navier-Stokes equations, *Comp. Meth. Appl. Mech. Engrg.*, 1982, **32**, 199–259

8 Cantekin, M. E. and Westerink, J. J. Non-diffusive N + 2 degree Petrov-Galerkin methods for two-dimensional transient transport computations, *Int. J. Num. Meth. Engrg.*, to appear, 1989

9 Carey, G. Exponential upwinding and integrating factors for symmetrization, *Comm. Appl. Num. Meth.*, 1985, **1**, 57–60

10 Celia, M. A. and Herrera, I. Solution of general ordinary differential equations by a unified theory approach, *Numerical Methods for Partial Differential Equations*, **3**(2), 1987, 117–129

11 Celia, M. A., Herrera, I. and Bouloutas, E. T. Adjoint Petrov-Galerkin methods for multi-dimensional flow problems, *Finite Element Analysis in Fluids*, Chung and Karr (eds.) UAH Press, 1989, 965–970

12 Celia, M. A., Herrera, I., Bouloutas, E. and Kindred, J. S. A new numerical approach for the advective-diffusive transport equation, *Numerical Methods for Partial Differential Equations*, 1989, **5**, 203–226

13 Celia, M. A., Kindred, J. S. and Herrera, I. Contaminant transport and biodegradation: I. A numerical model for reactive transport in porous media, *Water Resources Research*, 1989, **25**, 1141–1148

14 Christie, I., Griffiths, D. F. and Mitchell, A. R. Finite element methods for second order differential equations with significant first derivatives, *Int. J. Num. Engrg.*, 1976, **10**, 1389–1396

15 Dahle, H. K., Espedal, M. S. and Ewing, R. E. Characteristic Petrov-Galerkin subdomain methods for convection diffusion problems, IMA Vol. 11, *Numerical Simulation in Oil Recovery*, M. F. Wheeler (ed.), Springer-Verlag, Berlin, 1988, 77–88

16 Dahle, H. K., Espedal, M. S., Ewing, R. E. and Saevareid, O. Characteristic adaptive sub-domain methods for reservoir flow problems, *Numerical Methods for Partial Differeential Equations*, to appear, 1989

17 Dawson, C. N., Russell, T. F. and Wheeler, M. F. Some improved error estimates for the modified method of characteristics, *SIAM J. Num. Anal.*, to appear, 1989

18 Demkowitcz, L. and Oden, J. T. An adaptive characteristic Petrov-Galerkin finite element method for convection-dominated linear and nonlinear parabolic problems in two space variables. *Comp. Meth. Appl. Mech. Engng.*, 1986, **55**, 63–87

19 Douglas, J. Jr. and Russell, T. F. Numerical methods for convection-dominated diffusion problems based on combining the method of characteristics with finite element or finite difference procedures, *SIAM J. Num. Anal.*, 1982, **19**, 871–885

20 Douglas, J. Jr., Martıńez-Gamba, and Squeff, M. C. J. Simulation of the transient behaviour of a one-dimensional semiconductor device, *Mat. Aplic. Comp.*, 1986, **5**, 103–122

21 Espedal, M. S. and Ewing, R. E. Characteristic Petrov-Galerkin subdomain methods for two-phase immiscible flow, *Comp. Meth. Appl. Mech. Engng.*, 1987, **64**, 113–135

22 Ewing, R. E. and Russell, T. F. Multistep Galerkin methods along characteristics for convection-diffusion problems, *Advances in Computer Methods for Partial Differential Equations* IV, Vichnevetsky and Stepleman, (eds.) IMACS, Rutgers Univ., 1981, 28–36

23 Ewing, R. E., Russell, T. F. and Wheeler, M. F. Convergence analysis of an approximation of miscible displacement in porous media by mixed finite elements and a modified method of characteristics, *Comp. Meth. Appl. Mech. Engng.*, 1984, **47**, 73–92

24 Hemker, P. W. *A Numerical Study of Stiff Two-Point Boundary Value Problems*, PhD Thesis, Mathematisch Centrum, Amsterdam, 1977

25 Herrera, I. *Boundary Methods: An algebraic theory*, Pitman Publishing Co., London, 1984

26 Herrera, I. Unified approach to numerical methods, Part I: Green's formula for operators in discontinuous fields, *Numerical Methods for Partial Differential Equations*, **1**(1), 1985, 25–44

27 Herrera, I. Unified approach to numerical methods, Part II: Finite elements, boundary elements, and their coupling, *Numerical Methods for Partial Differential Equations*, 1985, **1**(3), 159–186

28 Herrera, I., Chargoy, L. and Alduncin, G. Unified approach to numerical methods, Part III: Finite differences and ordinary differential equations, *Numerical Methods for Partial Differential Equations*, 1985, **1**(4), 241–258

29 Herrera, I. The algebraic theory approach for ordinary differential equations: highly accurate finite differences, *Numerical Methods for Partial Differential Equations*, 1987, **3**(3), 199–218

30 Herrera, I., Ewing, R. E., Russell, T. F. and Celia, M. A. Eulerian Lagrangian localized adjoint methods: Theoretical underpinnings, in preparation, 1989

31 Hervouet, J. M. Application of the method of characteristics in their weak formulation to solving two-dimensional advection equations on mesh grids, *Computational Techniques for Fluid Flow*, Vol. 5 of the series *Recent Advances in Numerical Methods in Fluids*, Taylor *et al.* (eds.) Pineridge Press, 1986, 149–185

32 Hughes, T. J. R. A simple scheme for developing 'upwind' finite elements, *Int. J. Num. Meth. Engng.*, 1978, **15**, 1359–1365

33 Hughes, T. J. R. and Brooks, A. A multidimensional upwind scheme with no crosswind diffusion, *Finite Element Methods for Convection Dominated Flows*, Hughes (ed.) AMD Vol. 34, ASME, 1979

34 Hughes, T. J. R. and Brooks, A. A theoretical framework for Petrov-Galerkin methods with discontinuous weighting functions: Applications to the streamline-upwind procedure, *Finite Elements in Fluids*, Vol. 4, Gallagher, *et al* (eds.) 47–65, 1982

35 Hughes, T. J. R. and Tezduyar, T. E. Finite element methods for first-order hyperbolic systems with particular emphasis on the compressible Euler equations, *Comp. Meth. Appl. Mech. Engng*. 1984, **45**, 217–284

36 Johnson, C. and Szepessy, A. On the covergence of a finite element method for a nonlinear hyperbolic conservation law, *Math. Comp.*, 1987, **49**, 427–444

37 Neuman, S. P. An Eulerian-Lagrangian numerical scheme for the dispersion-convection equation using conjugate space-time grids, *J. Comp. Phys.*, 1981, **41**, 270–294

38 Neuman, S. P. Adaptive Eulerian-Lagrangian finite element method for advection-dispersion, *Int. J. Num. Meth. Engng*, 1984, **20**, 321–337

39 Neuman, S. P. and Sorek, S. Eulerian-Lagrangian methods for advection-dispersion, *Proc. Fourth Int. Conf. Finite Elements in Water Resources*, Holz *et al.* (eds.) Springer-Verlag, 1982, 14.41-14.68

40 Pinder, G. F. and Cooper, H. H. A numerical technique for calculating the transient position of the saltwater front, *Water Resources Research*, 1970, **6**(3) 875–882

41 Pinder, G. F. and Gray, W. G. *Finite Element Simulation in Surface and Subsurface Hydrology*, Academic Press, New York, 1977

42 Pironneau, O. On the transport-diffusion algorithm and its application to the Navier-Stokes equations, *Numer. Math.*, 1982, **38**, 309–332

43 Russell, T. F. Eulerian-Lagrangian localized adjoint methods for

advection-dominated problems, *Proc. 13th Dundee Biennial Conf. on Numerical Analysis*, Research Notes in Mathematics Series, Pitman, to appear, 1989

44 Russell, T. F. Time stepping along characteristics with incomplete iteration for a Galerkin approximation of miscible displacement in porous media, *SIAM J. Num. Anal.*, 1985, **22**, 970–1013

45 Russell, T. F., Wheeler, M. F. and Chiang, C. Y. Large-scale simulation of miscible displacement by mixed and characteristic finite element methods, *Mathematical and Computational Methods in Seismic Exploration and Reservoir Modeling,*, Fitzgibbon (ed.) SIAM, Philadelphia, 1986, 85–107

46 Tezduyar, T. E. and Ganjoo, D. K. Petrov-Galerkin formulations with weighting functions dependent upon spatial and temporal discretization: Application to transient convective-diffusion problems, *Comp. Meth. Appl. Mech. Engng.*, 1986, **59**, 49–71

47 Varoglu, E. and Finn, W. D. L. Finite elements incorporating characteristics for one-dimensional diffusion-convection equation, *J.l Comp. Phys.*, 1980, **34**, 371–389

48 Westerink, J. J. and D. Shea, Consistent higher degree Petrov-Galerkin methods for the solution of the transient convection-diffusion equation, *Int. J. Num. Meth. Engng.*, to appear, 1989

49 Wheeler, M. F. and Dawson, C. N. An operator-splitting method for advection-diffusion-raction problems, *MAFELAP Proceedings*, Vol. VI, Whiteman, J. A. (ed.) Academic Press, 1988, 463–482

APPENDIX

This appendix presents the ELLAM approximating equations for the case of general Courant number. Let $\mathrm{Cu} \equiv (V(\Delta t)/\Delta x)$ denote the Courant number, with $Nc \leq \mathrm{Cu} < Nc + 1$, Nc integer. Let constant spacing be assumed, so that $x_i = i(\Delta x)$. Also let $\Omega_x = [0, l]$, with $x_0 = 0$, $x_E = l$. Equations are presented below for the following test functions: (1) $w_0^{n+1}(x, t)$; (2) $w_i^{n+1}(x, t)$, $1 \leq i < Nc$; (3) $w_{Nc}^{n+1}(x, t)$; (4) $w_{Nc+1}^{n+1}(x, t)$; (5) $w_i^{n+1}(x, t)$, $Nc + 1 < i < E$; (6) $w^{**}(x, t) \equiv \Sigma_{i=E}^{E+Nc} w_i^{n+1}(x, t)$ (See Section 5). Only equations associated with test functions of class (5) are devoid of boundary influences; all others are influenced by either inflow or outflow boundaries. Fig. A.1 illustrates the characteristics of interest. The equations that follow are written under the assumption that $Nc < E - 1$.

Case 1: $w_0^{n+1}(x, t)$

$$\int_{x_0}^{x_1} u(x, t^{n+1}) w_0^{n+1}(x, t^{n+1})\, dx - V\int_{t_1^*}^{t^{n+1}} u(0, t) w_0^{n+1}(0, t)\, dt - D\left[\left(\frac{-1}{\Delta x}\right)\int_{t_1^*}^{t^{n+1}} u(0, t)\, dt + \left(\frac{1}{\Delta x}\right)\int_{t_1^*}^{t^{n+1}} u(x_r^0(t), t)\, dt\right] + D\int_{t_1^*}^{t^{n+1}} \frac{\partial u}{\partial x}(0, t) w_0^{n+1}(0, t)\, dt = \int_{\Omega_2^0} f(x, t) w_0^{n+1}(x, t)\, dx\, dt. \quad \text{(A.1)}$$

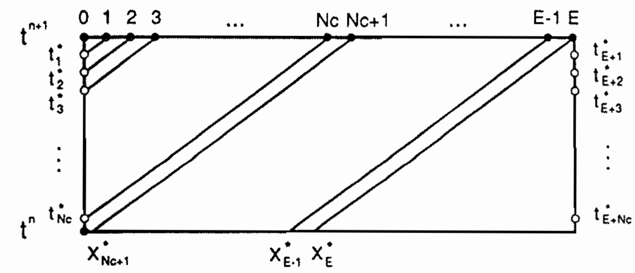

Fig. A.1. Geometry of ELLAM approximations for arbitrary Courant number

Note: if $Nc = 0$, t_1^* is replaced by t^n and $V\int_{t_1^*}^{t^{n+1}} u(0, t) w_0^{n+1}(0, t)\, dt$ is replaced by

$$\left[V\int_{t^n}^{t^{n+1}} u(0, t) w_0^{n+1}(0, t)\, dt + \int_{x_0}^{x_1^*} u(x, t^n) w_0^{n+1}(x, t^n)\, dx\right].$$

Case 2: $w_i^{n+1}(x, t)$, $1 \leq i \leq Nc$ (Note: If $Nc = 0$ or 1, no equations are written).

$$\int_{x_{i-1}}^{x_{i+1}} u(x, t^{n+1} w_i^{n+1}(x, t^{n+1})\, dx - V\int_{t_{i+1}^*}^{t_{i-1}^*} u(0, t) w_i^{n+1}(0, t)\, dt - D\left[\left(\frac{1}{\Delta x}\right)\int_{t_{i-1}^*}^{t^{n+1}} u(x_l^i(t), t)\, dt - \left(\frac{2}{\Delta x}\right)\int_{t_i^*}^{t^{n+1}} u(x_c^i(t), t)\, dt + \left(\frac{1}{\Delta x}\right)\int_{t_{i+1}^*}^{t^{n+1}} u(x_r^i(t), t)\, dt\right] + D\int_{t_{i+1}^*}^{t_{i-1}^*} \frac{\partial u}{\partial x}(0, t) w_i^{n+1}(0, t)\, dt - D\left(\frac{1}{\Delta x}\right)\left[\int_{t_i^*}^{t_{i-1}^*} u(0, t)\, dt - \int_{t_{i+1}^*}^{t_i^*} u(0, t)\, dt\right] = \int_{\Omega_1^i} f(x, t) w_i^{n+1}(x, t)\, dx\, dt + \int_{\Omega_2^i} f(x, t) w_i^{n+1}(x, t)\, dx\, dt \quad \text{(A.2)}$$

where $t_0^* = t^{n+1}$.

Case 3: $w_{Nc}^{n+1}(x, t)$

$$
\begin{aligned}
&\int_{x_{Nc-1}}^{x_{Nc+1}} u(x, t^{n+1}) w_{Nc}^{n+1}(x, t^{n+1})\, dx \\
&\quad - \left[\int_{x_0}^{x^*_{Nc+1}} u(x, t^n) w_{Nc}^{n+1}(x, t^n)\, dx + V \int_{t^n}^{t^*_{Nc-1}} u(0, t) w_{Nc}^{n+1}(0, t)\, dt \right] \\
&\quad - D\left[\left(\frac{1}{\Delta x}\right) \int_{t^*_{Nc-1}}^{t^{n+1}} u(x_l^{Nc}(t), t)\, dt - \left(\frac{2}{\Delta x}\right) \int_{t^*_{Nc}}^{t^{n+1}} u(x_c^{Nc}(t), t)\, dt + \left(\frac{1}{\Delta x}\right) \int_{t^n}^{t^{n+1}} u(x_r^{Nc}(t), t)\, dt \right] \\
&\quad + D \int_{t^n}^{t^*_{Nc-1}} \frac{\partial u}{\partial x}(0, t) w_{Nc}^{n+1}(0, t)\, dt \\
&\quad - D\left(\frac{1}{\Delta x}\right) \left[\int_{t^*_{Nc}}^{t^*_{Nc-1}} u(0, t)\, dt - \int_{t^n}^{t^*_{Nc}} u(0, t)\, dt \right] \\
&= \int_{\Omega_1^{Nc}} f(x, t) w_{Nc}^{n+1}(x, t)\, dx\, dt \\
&\quad + \int_{\Omega_2^{Nc}} f(x, t) w_{Nc}^{n+1}(x, t)\, dx\, dt. \qquad \text{(A.3)}
\end{aligned}
$$

Case 4: $w_{Nc+1}^{n+1}(x, t)$

$$
\begin{aligned}
&\int_{x_{Nc}}^{x_{Nc+2}} u(x, t^{n+1}) w_{Nc+1}^{n+1}(x, t^{n+1})\, dx \\
&\quad - \left[\int_{x_0}^{x^*_{Nc+2}} u(x, t^n) w_{Nc+1}^{n+1}(x, t^n)\, dx + V \int_{t^n}^{t^*_{Nc}} u(0, t) w_{Nc+1}^{n+1}(0, t)\, dt \right] \\
&\quad - D\left[\left(\frac{1}{\Delta x}\right) \int_{t^*_{Nc}}^{t^{n+1}} u(x_l^{Nc+1}(t), t)\, dt - \left(\frac{2}{\Delta x}\right) \int_{t^n}^{t^{n+1}} u(x_c^{Nc+1}(t), t)\, dt + \left(\frac{1}{\Delta x}\right) \int_{t^n}^{t^{n+1}} u(x_r^{Nc+1}(t), t)\, dt \right] \\
&\quad + D \int_{t^n}^{t^*_{Nc}} \frac{\partial u}{\partial x}(0, t) w_{Nc+1}^{n+1}(0, t)\, dt \\
&\quad - D\left(\frac{1}{\Delta x}\right) \int_{t^n}^{t^*_{Nc}} u(0, t)\, dt \\
&= \int_{\Omega_1^{Nc+1}} f(x, t) w_{Nc+1}^{n+1}(x, t)\, dx\, dt \\
&\quad + \int_{\Omega_2^{Nc+1}} f(x, t) w_{Nc+1}^{n+1}(x, t)\, dx\, dt. \qquad \text{(A.4)}
\end{aligned}
$$

Case 5: $w_i^{n+1}(x, t)$, $Nc - < i < E$

$$
\begin{aligned}
&\int_{x_{i-1}}^{x_{i+1}} u(x, t^{n+1}) w_i^{n+1}(x, t^{n+1})\, dx \\
&\quad - \int_{x^*_{i-1}}^{x^*_{i+1}} u(x, t^n) w_i^{n+1}(x, t^n)\, dx \\
&\quad - D\left[\left(\frac{1}{\Delta x}\right) \int_{t^n}^{t^{n+1}} u(x_l^i(t), t)\, dt - \left(\frac{2}{\Delta x}\right) \int_{t^n}^{t^{n+1}} u(x_c^i(t), t)\, dt + \left(\frac{1}{\Delta x}\right) \int_{t^n}^{t^{n+1}} u(x_r^i(t), t)\, dt \right] \\
&= \int_{\Omega_1^i} f(x, t) w_i^{n+1}(x, t)\, dx\, dt \\
&\quad + \int_{\Omega_2^i} f(x, t) w_i^{n+1}(x, t)\, dx\, dt. \qquad \text{(A.5)}
\end{aligned}
$$

Case 6: $w^{**}(x, t) \equiv \Sigma_{i=E}^{E+Nc+1} w_i^{n+1}(x, t)$ (Note: $w^{**} = 1$ on $\Omega_2^{**} \equiv \Omega_2^E U \Omega_2^{E+1} U \ldots U \Omega_2^{E+Nc+1}$)

$$
\begin{aligned}
&\int_{x_{E-1}}^{x_E} u(x, t^{n+1}) w_E^{n+1}(x, t^{n+1})\, dx \\
&\quad - \int_{x^*_{E-1}}^{x_E} u(x, t^n) w^{**}(x, t^n)\, dx \\
&\quad - D\left[\left(\frac{1}{\Delta x}\right) \int_{t^n}^{t^{n+1}} u(x_l^E(t), t)\, dt - \left(\frac{1}{\Delta x}\right) \int_{t^n}^{t^{n+1}} u(x_c^E(t), t)\, dt \right. \\
&\quad \left. + V \int_{t^n}^{t^{n+1}} u(l, t)\, dt - D \int_{t^n}^{t^{n+1}} \frac{\partial u}{\partial x}(l, t)\, dt \right] \\
&= \int_{\Omega_1^E} f(x, t) w^{**}(x, t)\, dx\, dt \\
&\quad + \int_{\Omega_2^{**}} f(x, t)\, dx\, dt. \qquad \text{(A.6)}
\end{aligned}
$$